Characterizing US contact patterns relevant to respiratory transmission from a pandemic to baseline: Analysis of a large cross-sectional survey

Juliana C. Taube, AB[1,], Zachary Susswein, BS[1], Dr. Vittoria Colizza, PhD[2], and Prof. Shweta Bansal, PhD[1,*]

[1]Department of Biology, Georgetown University, Washington, DC, USA
[2]INSERM, Paris, France
[*]Corresponding Author, shweta.bansal@georgetown.edu

December 2024

Abstract

Background: Contact plays a critical role in infectious disease transmission. Characterizing heterogeneity in contact patterns across individuals, time, and space is necessary to inform accurate estimates of transmission risk, particularly to explain superspreading, predict age differences in vulnerability, and inform social distancing policies. Current respiratory disease models often rely on data from the 2008 POLYMOD study conducted in Europe, which is now outdated and potentially unrepresentative of behavior in the US. We seek to understand the variation in contact patterns across time, spatial scales, and demographic and social classifications, and what social behavior looks like at baseline in the absence of an ongoing pandemic.

Methods: We analyze spatiotemporal non-household contact patterns across 10.7 million survey responses from June 2020 - April 2021 post-stratified on age and gender to correct for sample representation. To characterize spatiotemporal heterogeneity in respiratory contact patterns at the county-week scale, we use generalized additive models. In the absence of non-pandemic US contact data, we employ a regression approach to estimate baseline contact and address this gap.

Findings: Although contact patterns varied over time during the pandemic, contact is relatively stable after controlling for disease. We find that the mean number of non-household contacts is spatially heterogeneous regardless of disease. There is additional heterogeneity across age, gender, race/ethnicity, and contact setting, with mean contact decreasing with age and lower in women. The contacts of White individuals and contacts at work or social events change the most under increased national incidence.

Interpretation: We develop the first county-level estimates of non-pandemic contact rates for the US that can fill critical gaps in parameterizing future disease models. Our results identify that spatiotemporal, demographic, and social heterogeneity in contact patterns is highly structured, informing the risk landscape of respiratory infectious disease transmission in the US.

Funding: Research reported in this publication was supported by the National Institutes of Health under award number R01GM123007 and R35GM153478 (SB).

Research in Context

Evidence before this study: We searched Google Scholar for contact data in the US both during and prior to the pandemic published by February 1, 2024 with the search terms "contact patterns", "social contact data", "disease-relevant contacts", "change in contacts pandemic", "urban rural social contacts," and "seasonality in contact patterns". We reviewed the bibliographies of these articles and included known literature not found via these search criteria. We excluded studies using mobility data, focusing on children, or excluding the United States. Previous work has been limited to the state scale or subsets of counties (e.g., focused on a few cities, a single state, or a few counties within a state) rather than all counties in the US.

Added value of this study: We contribute the first high-resolution pandemic contact estimates for the US and infer non-pandemic contact patterns at fine spatial and temporal scales. Our results indicate that the number of contacts is fairly stable over time in the absence of major disease, suggesting that the number of contacts is not a primary driver of respiratory infectious disease seasonality in the US. We also identify groups at greatest disease risk due to higher contacts, including younger adults, men, and Hispanic and Black individuals.

Implications of all the available evidence: This study demonstrates the importance of incorporating age-specific and spatial heterogeneity of contact patterns into future disease models to build accurate estimates of transmission risk. We demonstrate that temporal variability in contact patterns is insufficient to drive respiratory infectious disease seasonality, that adaptive behaviors in response to disease shift risk along an urban-rural gradient, and that some vulnerable groups are at increased risk of exposure due to contact. We advocate that geographic and social heterogeneity in exposure to disease due to contact patterns be captured more comprehensively for accurate infectious disease predictions and effective and equitable disease mitigation.

Introduction

Respiratory infectious disease transmission via direct or droplet routes requires close contact. Research over the last two decades has demonstrated that human contact patterns are highly variable between individuals and across geography [1, 2] and highlighted the consequences of this variability for epidemic outcomes and dynamics [3]. Yet, to date, detailed empirical data on contact patterns across the United States have not been available. This lack of data leaves several important gaps in our understanding of the drivers of disease transmission. For example, we'd like to know what factors (e.g., age, season, or location) influence contact patterns across the US and how these factors contribute to variability in infection risk. This information is essential to design targeted interventions and generate accurate estimates of transmission risk across individuals, space, and time. With a new dataset composed of over 10 million survey responses from June 2020 through April 2021, we developed the first detailed characterization of heterogeneities in human contact patterns across the US.

Most infectious disease models assume homogeneous mixing amongst individuals. That is, all individuals have the same contact rate and ability to transmit disease. Homogeneous mixing models have transformed the prediction and control of disease outbreaks (e.g., through R_t estimation [4]) but produce different epidemic dynamics and outcomes than models that incorporate heterogeneities in contact patterns [3, 5]. The POLYMOD study published in 2008 was the first extensive survey to characterize heterogeneities in routine contact patterns relevant to respiratory infectious disease transmission. The data, from eight European countries, suggested that individual contact rates are not homogeneous but rather heavy-tailed and highly assortative by age [1]. These estimates have been used to understand epidemic dynamics, design vaccine strategies, and predict intervention outcomes (e.g., [6–10]). However, the POLYMOD estimates did not capture dynamic behavior in the presence of disease. To fill this gap, researchers conducted the CoMix study during the COVID-19 pandemic to collect contact data contemporaneous with disease across Europe [11, 12]; estimates from the survey were incorporated into forecasting efforts in the UK with mixed results [13]. Notably, both surveys failed to capture fine-scale temporal variability or social heterogeneity in contact and may not be representative of behavior in the United States.

Beyond individual heterogeneity, there are several meaningful dimensions across which contact patterns may vary. Spatial heterogeneity in human behavior plays a vital role in disease dynamics (e.g., [14–17]); if contact patterns exhibit spatial heterogeneity, that might explain observed hotspots of disease burden and/or dynamics of disease spread. Likewise, changes in contact patterns over time may contribute to respiratory infectious disease seasonality (e.g., [18, 19]). Contact may also vary based on surrounding disease transmission as individuals shift their behavior to mitigate risk. These potential heterogeneities in contact patterns profoundly affect our understanding and prediction of epidemic dynamics and our ability to target behavioral interventions. Yet little empirical data exists on them. To identify the dimensions across which contact meaningfully varies, we need high-resolution contact data across geography, time, demography, social classifications, and in the context of disease transmission.

Recent attention has been given to contact patterns in the US, resulting in several studies published over the past few years (in addition to small/indirect earlier studies [20, 21]) which provide insights into variations in contact patterns across multiple dimensions. Breen et al. [22] demonstrate that contact varies between states but are unable to characterize spatial heterogeneity at finer scales in the US, even though other public health-related behaviors have been demonstrated to vary at the county-level [23, 24]. Dorelien et al. [25] use time-use surveys to demonstrate that contact between urban and rural areas may not differ despite the perception that urban inhabitants have more contacts. On temporal variation in contact, one pre-pandemic study found no variation in adult contacts over time [25], while another observed changes from September to May [20]. Many studies find that contact is higher in younger adults, men, and non-White populations, although which race/ethnicity group has the highest contact depends on the study [20, 26–28]. Because these past studies are limited in sample size or resolution, they are constrained in their ability to comprehensively characterize heterogeneities in contact patterns across space, time, and social groups.

Now that the US COVID-19 public health emergency has ended, it is vital to characterize contact patterns

during the pandemic but also under non-pandemic baseline conditions. In general, pandemic social distancing reduced overall contact (e.g., [29]). However, past work has demonstrated that adherence to pandemic social distancing was heterogeneous across populations, driven in part by health disparities and social inequities that affect the ability of individuals to engage in behavioral interventions [30] and by a patchwork of non-pharmaceutical interventions (e.g., school closures, work from home, gathering bans, mask requirements) implemented at a variety of spatial scales. For example, urban areas exhibited more significant reductions in mobility and, therefore, likely contact [31]. Individuals of higher socioeconomic status are known to have had greater flexibility in their mitigation behavior and could further reduce contacts. Understanding which groups and locations are at the highest infection risk during pandemics and seasonal epidemics is critical for targeted public health surveillance and resource allocation but requires detailed contact data disaggregated by location, age, gender, and race/ethnicity.

Here, we address these pressing gaps by developing fine-scale spatiotemporal estimates of mean non-household contacts in adults. We use an extensive national survey with over 10 million responses collected at the county level and correct for issues of representativeness and small sample size via post-stratification and generalized additive models. We characterize several heterogeneities in contact patterns throughout the pandemic and infer non-pandemic contact patterns by controlling for the effect of disease. We focus on four central questions: (1) How does mean contact vary over time? (2) How does mean contact vary across geography in urban versus rural settings? (3) How do contact patterns vary across age, gender, and race/ethnicity classifications? (4) What are contact patterns like at baseline? Our results are the most comprehensive high-resolution estimates of US contact patterns to date and can inform future disease models in the US, provide insight into local and temporal variation in behavior in response to public health messaging, and contribute to our understanding of drivers of respiratory infectious disease seasonality.

Methods

In this study, we seek to characterize heterogeneities in non-household contact patterns in the United States using survey data from June 2020 to April 2021. We use survey raking and reweighting of responses to correct for unrepresentative survey sampling. Due to the low sample size in some counties, we use generalized additive models (GAMs) to develop smoothed county-week estimates of the mean number of non-household contacts, disaggregated by geographic, demographic, and social categories. To interrogate whether there is temporal variability in US contact patterns in the absence of a pandemic, we account for the effect of disease incidence on contact with a simple linear regression model and examine the remaining unexplained variability in contact.

Survey data

We analyzed survey responses of the number of non-household contacts for all 50 US states and the District of Columbia using data from the US COVID-19 Trends and Impact Survey (CTIS) [32]. The CTIS was created by the Delphi Research Group at Carnegie Mellon University and distributed through a partnership with Facebook. Beginning in April 2020, a random state-stratified sample of active Facebook users were invited daily to take the survey about COVID-19 and report how many people they had direct contact with outside their household, where contact was defined as "a conversation lasting more than 5 minutes with a person who is closer than 6 feet away from you, or physical contact like hand-shaking, hugging, or kissing." Contacts were disaggregated by settings outside the home in the survey question: work, shopping for groceries or other essentials, social gatherings, or other. We analyze the sum of contacts across all these settings starting in June 2020. We removed responses with more than 72 contacts in the last 24 hours (the 95th percentile) and performed sensitivity analyses of this truncation point (Figures S41 to S44). Age, gender, and race were self-reported in the survey, and the survey data are representative of the US population by age, sex, and race/ethnicity (Table S1). To adjust for unrepresentative sampling at the county-scale, we generated response weights to match county age and sex distributions and post-stratified the data (details in supplement). As

race/ethnicity is not available throughout the full study period, we cannot include it in the raking procedure for all estimates. To test the sensitivity of our estimates to including race/ethnicity in the raking weights, we compared mean contact estimates at the state-month level for September 2020 - April 2021 (Figure S35). We additionally account for race/ethnicity in the raking weights for any race/ethnicity-specific analyses.

County urbanicity was determined using the NCHS 2013 urban-rural classifications, where 1 indicates large central metropolitan areas, and 6 represents rural non-core areas [33].

Spatiotemporal contact estimation

To address weekly noise and low sample sizes in the data, we estimated smoothed county-week mean non-household contacts with hierarchical generalized additive models (GAMs). We use penalized thin-plate splines weighted by sample size with a weekly smooth for each state and a factor smooth for each county within the state, with shared smoothness parameters across counties. Thus, information is shared within states but not between; estimates are penalized to the state average, which may be biased towards urban counties. The model is structured as:

$$\text{mean contact}_i = \beta_0 + f_s(t) + f_i(t) + \epsilon_i$$

where

$$f_j(t) = \sum_{k=1}^{K} \beta_{j,k} b_{j,k}(t)$$

where f_j represents the penalized smoothing function of interest, with j as state s or county i level, and t represents each week [34]. The coefficients $\beta_{j,k}$ are estimated for each of the K basis functions $b_{j,k}$.

We fit separate GAMs to estimate contact by age, gender, race/ethnicity, and setting at the county or state level for pandemic conditions. Additional details can be found in the supplement.

Baseline contact estimation

To estimate contact in the absence of a pandemic, we used a linear regression model of weekly contact (as modeled using the GAMs above) predicted by national case incidence [35], state-level policy stringency (measured via the Oxford Stringency Index [36]), county-level policy stringency (calculated as the sum of various ordinal county policies [37–43]), and percentage of the county vaccinated for COVID-19 [24] (Figure S31). We propose that behavioral modification due to risk perception is mediated by disease incidence; to test this, we also considered a subjective measure of risk perception (based on a different question from the CTIS), and find it to be less predictive than incidence (Table S2). We also considered the role of incidence information across scales (county, state, and national) and found state and national scales to be highly collinear, and county incidence to be less informative relative to national incidence (Table S2). The Oxford Stringency Index captures the extent of policy limitations on human behavior, including school, work, and transit closures, stay at home requirements, and travel restrictions [36] at the state level. County-level restaurant and bar closures, mask mandates, gathering bans, and stay at home orders compose the county policy variable. (Additional sensitivity analyses related to the policy variables can be found in Figures S46 and S47). We hypothesized that increases in disease incidence would lead to a linear decrease in contact rates, which is supported by the survey data (Figures S28, S29). The model is as follows:

$$\begin{aligned}\text{mean contact}_{i,t} = \beta_{0,i} + \beta_{1,i}\text{incidence}_{n,t} + \beta_{2,i}\text{percent vaccinated}_{i,t} + \beta_{3,i}\text{policy index}_{s,t} + \\ \beta_{4,i}\text{policy index}_{i,t} + \beta_{5,i}\text{incidence}_{n,t} * \text{percent vaccinated}_{i,t} + \epsilon_{i,t}\end{aligned}$$

where i represents each county, s each state, and n the nation, t represents each week, incidence_n represents the 4-week rolling average (mean of the previous three weeks and the current week) of national incident

cases, policy index$_s$ represents the Oxford Stringency Index centered at the minimum value observed in the regression period for each state, policy index$_c$ represents the sum of county level policy metrics centered at the minimum value observed in the regression period for each county, and $\epsilon \sim N(0, \sigma^2)$. Note that counties are not pooled together which allows us to capture differences in county-level responses to disease and policy metrics. Additional model selection details can be found in the supplement (Table S2).

Contact after controlling for disease was defined as

$$\text{baseline contact}_{i,t} = \phi_i \ (\beta_{0_i} + \epsilon_{i,t})$$

where

$$\phi_i = \frac{\omega_{2019,i}}{\omega_{2020,i}}$$

and $\omega_{y,i}$ is defined as the mean number of trips into or within a given county i for October thru December of year y. We added the residual to account for temporal changes in contact not captured by the incidence and policy data. The mobility data is obtained from the SafeGraph Social Distancing dataset [44]. We scale by pre-pandemic mobility data to account for the drastic decrease in contact upon SARS-CoV-2 introduction in the United States. While mobility data do not directly measure contact, they are a reasonable proxy for contact as they are highly correlated (Figure S27).

We fit separate regressions to estimate contact by age, gender, race/ethnicity, and setting at the county or state level for non-pandemic conditions. These models allow us to estimate baseline contact for each demographic/social group by estimating the effect of (overall disease-mediated) risk perception and policy to vary by group.

This analysis was limited to the period from October 2020 to April 2021 to encompass a full "wave" of COVID-19 in the US. Diagnostics for these regression models are provided in the supplement (Figures S36 to S39).

Role of the funder

The funder had no role in data collection, analysis, interpretation, writing of the manuscript nor the decision to submit. JCT, ZS, and SB had access to all of the data. All authors were responsible for the decision to submit the manuscript.

Results

We characterized heterogeneities in average daily contact patterns at the county-week scale from June 2020 through April 2021 in the United States using 10.7 million valid responses from the CTIS [32] (Figures S20, S21). The survey uses a well-established definition of contact relevant to respiratory disease transmission, and thus offers an advantage over GPS location-based mobility data to characterize contact patterns; past work has also demonstrated that social contact data is more predictive of transmission than mobility data [45–47]. We focus on non-household contacts as they play a crucial role in the dynamics of casual contact infections [48]. To explore variability in contact patterns over time, particularly during the autumn-to-spring period when seasonal changes are expected [49], we developed a statistical model. Rather than capturing all sources of heterogeneity, our model aims to parsimoniously account for pandemic-related effects to estimate non-pandemic contact patterns. We hypothesize that if disease incidence-mediated risk perception and intervention-related behavior change fully explain temporal variability in contact, then baseline behavior remains temporally stable.

Contact is stable under baseline conditions

Contact varies across the pandemic period, although most counties exhibit similar contact dynamics: increased contact during summer 2020 and spring 2021 and decreased contact during winter 2020-21 (Figure 1A). Some counties, predominantly in Florida, Arizona, Texas, and other parts of the southern US, also reduced their contact in the summer of 2020, coinciding with a COVID-19 surge in the region. This variation appears to be inversely related to SARS-CoV-2 incidence.

We explore this association using regression models with national case incidence, state and county policies, and county vaccination coverage to predict contact from October 2020 to April 2021. After controlling for the effect of disease on behavior, contact is temporally stable across counties (Figure 1B). Remaining fluctuations are neither substantial nor systematic.

We also validate predicted trends in baseline contact after the Omicron wave by using a different question on the CTIS about contact avoidance (Figures S51 and S53). Therefore, our baseline contact estimates can be interpreted as conservative predictions for non-pandemic contact beyond the acute phase of the COVID-19 pandemic.

Contact is geographically heterogeneous but structured by urbanicity

Mean non-household contact is spatially heterogeneous during the pandemic (Figure 2A) and in the absence of a pandemic (Figure 2B). During the pandemic, the highest degree of contact is observed across the central and southern US while the lowest contact rates are observed along the north Atlantic and western coasts. In contrast, under baseline conditions, we predict a change in the geographic pattern of contact rates.

We investigate these geographic patterns by considering the association with urbanicity. During the COVID-19 pandemic, respondents in the most urban US counties (NCHS class 1) tended to have fewer contacts compared to more rural counties (Figure 2C). This difference is eliminated by controlling for disease (Figure 2C), suggesting that individuals in urban counties are expected to have slightly more contacts than rural residents under this contact definition in non-pandemic situations.

We demonstrate that these results are robust to truncation in the reported number of contacts (Figures S41 to S44).

Contact varies demographically and socially

Contact also varies across demographic and social classifications during the pandemic and at baseline. Older respondents tend to have fewer contacts, with individuals between 18 and 54 reporting about the same numbers of contacts on average across the study period (Figures 3A, S48). Men tend to have more contacts than women (Figure 3B), whereas Hispanic respondents have the most contacts compared to Asian respondents who have the fewest (Figure 3C). Most adult contacts occur in work settings, followed by shopping for essentials (Figure 3D). Using separate regression models and county-specific mobility data, we infer baseline contact for each social category. While responsiveness to disease incidence varies within social classifications (Figure S33), the relationship between baseline contact and each social classification remains the same as during the pandemic (Figure 3). Our baseline results are consistent with those from other studies (Figures S1 to S4). During the pandemic, contact estimates are more variable across studies, potentially due to differences in contact definition, survey design, or survey period (Figures S5 to S19).

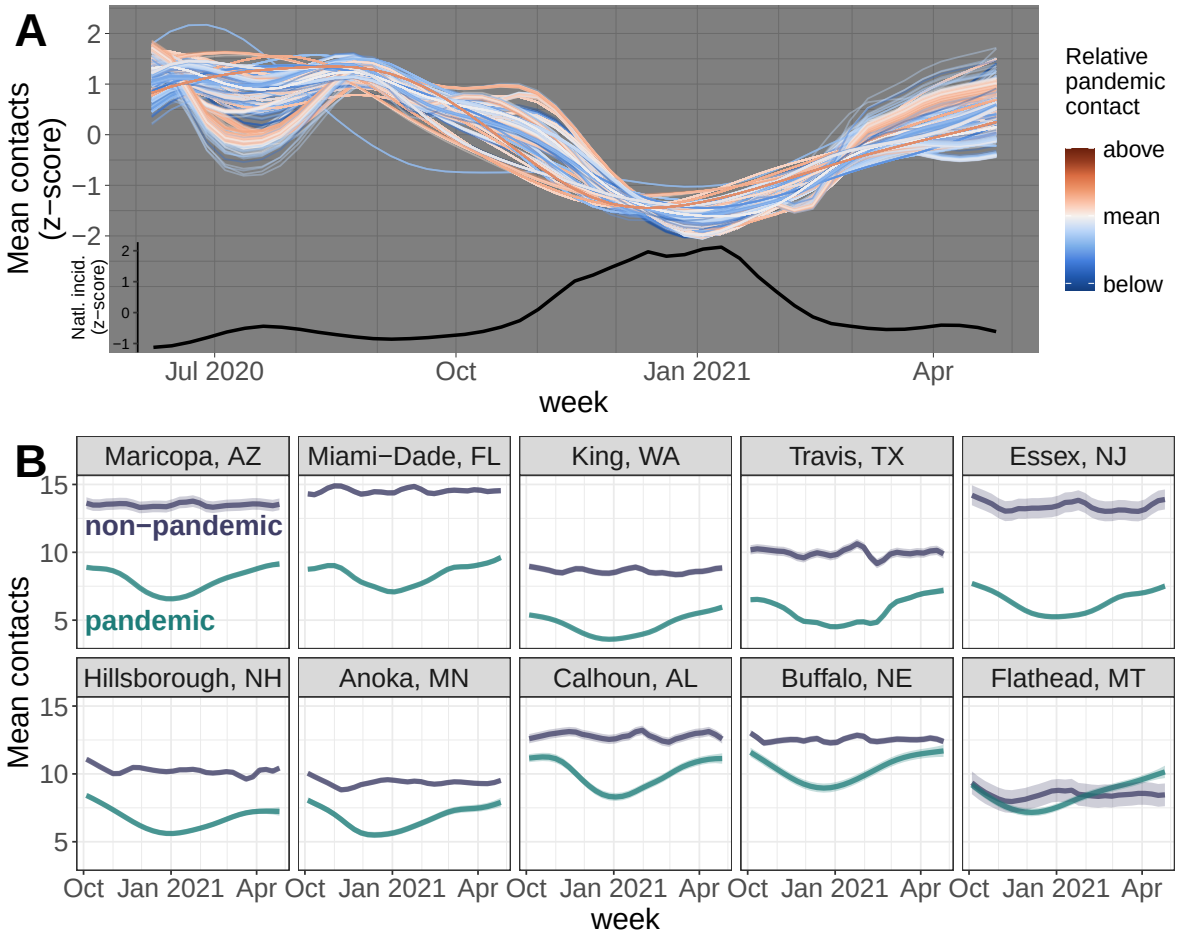

Figure 1. Counties have similar contact dynamics over time and relatively stable contact after controlling for disease. (A) Most counties had higher contact during the summer of 2020, and all had lower contact during the winter of 2020-21. Counties that experienced a dip in contact in the summer of 2020 were typically in states that exhibited higher incidence during that time. Each line represents a county colored by mean contact relative to the national mean (above or below); zscored contact relative to each county's mean is shown to allow comparison between time series despite the large range of mean contact values across counties. Black line shows the z-score of centered 3-week rolling average of national case incidence for context. (B) Contact in the absence of disease (slate) is effectively constant over time compared to observed contact during the pandemic (teal) across a diverse set of counties. We controlled for disease using a linear regression predicting contact from national case incidence, state and county policy data, and county vaccination coverage. This analysis is restricted to October 2020 to April 2021 to encompass a full wave of COVID-19. Shaded areas represent one standard error above and below the fitted contact value or estimated non-pandemic value.

Discussion

Interpersonal contact is required for the spread of directly-transmitted pathogens such as SARS-CoV-2. Nevertheless, contact patterns remain poorly understood and difficult to predict. Previous contact studies have focused on European nations and measured contact at coarse spatial and temporal scales (e.g., [1,22,28, 50]). These broad scopes leave open questions about how contact patterns vary subnationally, across seasons, and between demographic and social classifications. Here, we estimate non-household contacts at the county-week scale in the US using responses from a large national survey during the COVID-19 pandemic (June

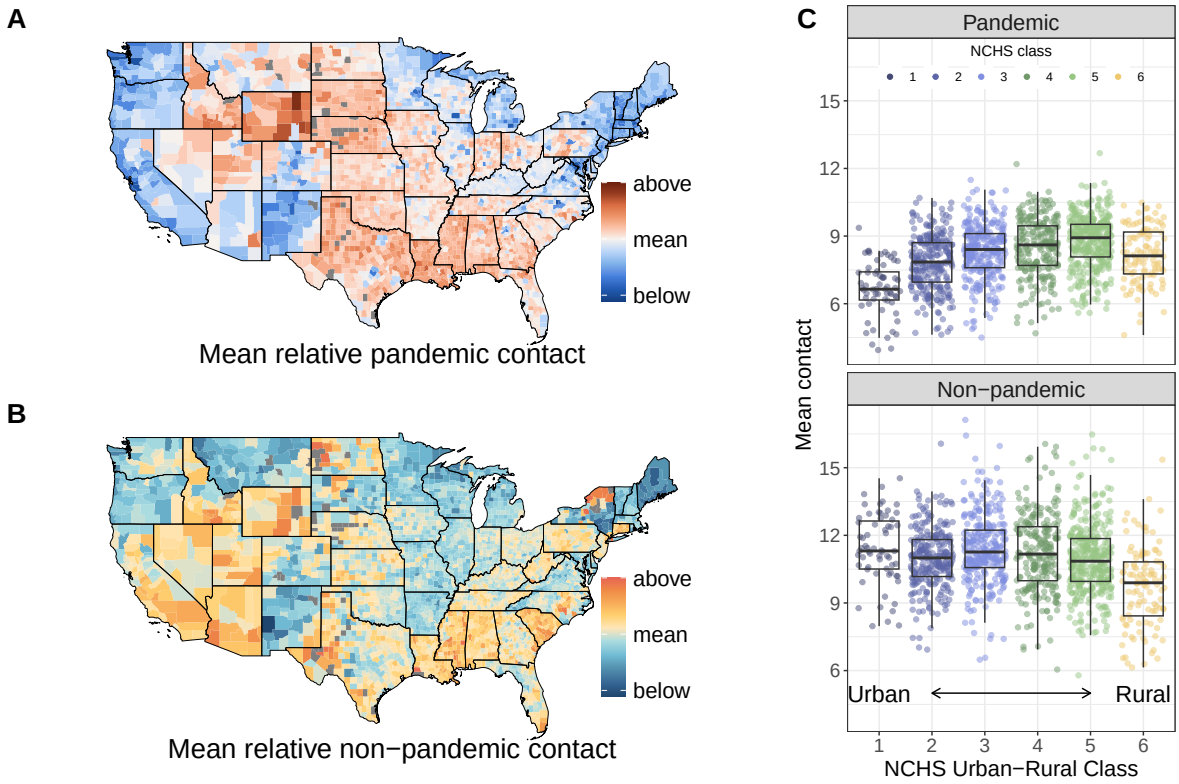

Figure 2. Contact is spatially heterogeneous regardless of disease incidence, but the urban-rural gradient reverses after controlling for disease incidence. (A) Map of mean number of non-household contacts per county relative to the national mean (8.7 contacts) during the pandemic (October 2020 - April 2021). There is high spatial heterogeneity in contact, even within states, which is fairly consistent across time (Figure S34). Gray counties did not have sufficient sample size to estimate contact. (B) Map of inferred mean number of non-household contacts per county relative to the national mean (10.9 contacts) in a non-pandemic scenario. Spatial heterogeneity in contact remains high, though which counties are above and below the national mean has shifted from the pattern observed during the pandemic. (C) Mean number of contacts for each county decreases with increasing urbanicity during the pandemic but increases with urbanicity during inferred non-pandemic times. Only counties with 10 or more responses per week each week (Oct 2020 - Apr 2021) are included.

2020 - April 2021). We used post-stratification and generalized additive models weighted by sample size to address sample representation and size issues. We compare our findings to a number of smaller past studies and show consistent patterns. We also use a regression approach to infer non-pandemic contact patterns by controlling for the effect of disease and pandemic interventions. Our findings have several implications for public health researchers and policymakers and can facilitate the much-needed improvement of future disease models and interventions in the US.

We find that most US communities exhibited similar temporal dynamics during the early COVID-19 pandemic which demonstrate an inverse relationship with disease trends. Indeed, after controlling for the effect of incidence-mediated risk perception and disease-related policy, we observe little variability in contact patterns over time suggesting that changes in numbers of contacts cannot explain respiratory infectious disease seasonality. As such, the role of contact in disease seasonality warrants further study; longer-term work should investigate whether these trends remain over multiple years and be used to validate our inferences. Importantly, the survey question we use did not differentiate between indoor and outdoor contact or whether individuals were wearing masks; the setting of human contact certainly affects the likelihood of transmission and has been shown to be seasonal [49]. Thus, with the data presented here, we hypothesize that the setting

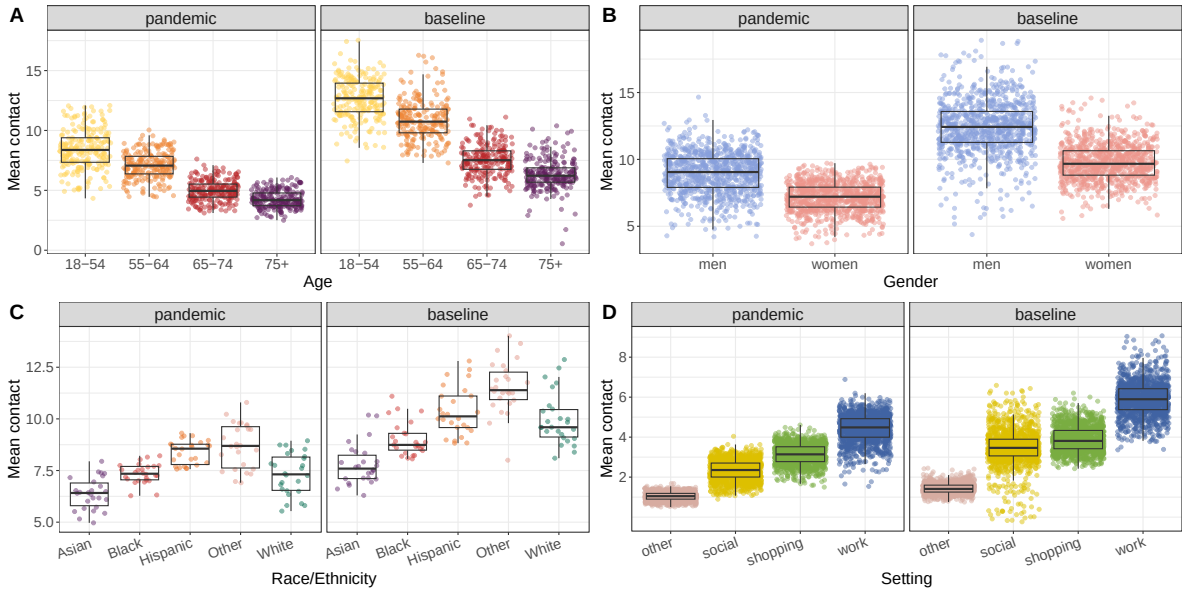

Figure 3. Contact varies across age, gender, race/ethnicity, and setting during the pandemic and at baseline. (A) Mean pandemic and baseline contact by age. Each point represents a county-age category. Analysis is limited to counties with 5+ responses per age category per week. (B) Mean pandemic and baseline contact by gender. Each point represents a county-gender category. Analysis is limited to counties with 5+ responses per gender category per week. (C) Mean pandemic and baseline contact by race/ethnicity. Each point represents a state-race/ethnicity category. Analysis is limited to states with 10+ responses per race/ethnicity category per week. All racial/ethnic categories are non-Hispanic unless labeled otherwise. Other denotes individuals who listed their race as American Indian, Alaska Native, Native Hawaiian, Pacific Islander, or "some other race". (D) Mean pandemic and baseline contact by setting. Each point represents a county-setting. Analysis is limited to counties with 10+ responses per setting per week.

of contact may be a larger driver of seasonality than the number of contacts. Our finding also reinforces other work that fine-grain temporal data may not be necessary for incorporating behavior into infectious disease models [51].

The high spatial heterogeneity in contact patterns that we observe allows us to identify areas at increased pandemic risk of transmission due to high contact rates, such as the central and southern US. This result also highlights the importance of high-resolution spatial data: there is high variability in contact within states that would be obscured if data are aggregated to the state level. We find that urban counties had fewer contacts on average during the pandemic; this is unsurprising given evidence that urban counties were more responsive to pandemic restrictions [26, 29, 31]. Under baseline conditions, however, we find that urban areas have more contacts on average than suburban or rural areas, which is consistent with behavioral heuristics based on population density. Earlier research has not found a consistent relationship between population density and contact rate, both outside the US [52–54] and in the US [25, 29]. This discrepancy may be explained by differences in contact definition; definitions that are tied to density are likely more representative of aerosol transmission. Given that geographic variation in disease risk creates challenges for disease surveillance, mitigation, and public health communication, further investigation on the role of spatial heterogeneity in behavior is warranted.

Understanding which groups have higher rates of contact is essential for the development of more targeted interventions and to address public health disparities stemming from structural inequities. While the nature of the CTIS precludes any analysis of contact assortativity or clustering, we can identify demographic and social classifications at greater risk due to higher contact rates. Indeed, degree has been shown to be the most important predictor of disease risk compared to other metrics [3]. Like other studies of smaller

sample size, both pre-pandemic and pandemic, we find that older adults have fewer contacts than younger adults [1, 27, 28, 55]. However, a limitation of our study (and most other contact studies) is a lack of data on children (individuals aged < 18). We also find that men have more contacts than women during the pandemic, as other national US surveys have shown [27, 28]. Our non-pandemic model shows that this difference persists in baseline conditions, in contrast with [20] (which may be a result of increased contacts by women in the home) and [1] (which finds no meaningful difference in contact between genders). Additionally, we found that Hispanic individuals had the highest contact rates during the pandemic and Asian respondents had the lowest; these results agree with a national survey in 2022 [28] but disagree with pre-pandemic time use data [25]. White respondents showed the most responsiveness to changes in disease incidence, likely reflecting increased ability to work from home. We note, however, that a lack of demographic/social group-specific mobility data may limit our inference of non-pandemic contact patterns across social categories, suggesting potential biases in our baseline contact estimates by social category (Figure S32). There may be additional biases in the data that we have not addressed, such as social desirability bias, over/under representation by political party, and underrepresentation of rural areas. Overall, our work highlights that social heterogeneities in contact patterns may be responsible for socially structuring transmission risks for respiratory infections and may shape the landscape of response to disease.

In summary, we have developed some of the most detailed pandemic and baseline estimates of contact patterns in the US to date which will be key to informing accurate estimates of transmission risk that account for spatial clustering. Our results can also aid the development of more efficiently targeted interventions. Our work highlights the value of collecting fine-scale behavioral data and the need for long-term longitudinal data collection on contact patterns in the US. We provide some of the first evidence that US adult contact patterns may not vary over time but do vary across counties, with ramifications for understanding respiratory infectious disease seasonality. Improving our understanding of contact patterns, which are such an integral component of disease transmission, should be further prioritized in research efforts going forward.

Contributors

JCT did the analyses, interpreted the findings, and drafted and edited the manuscript. ZS contributed to the analyses and edited the manuscript. VC interpreted the findings and edited the manuscript. SB conceived and supervised the study, interpreted the findings, and edited the manuscript. JCT, ZS, and SB accessed and verified the data.

Declaration of Interests

We declare no competing interests.

Data sharing

Contact estimates, both during the pandemic and at baseline, at the county-week scale and all code to produce and analyze these data will be made available on GitHub at `https://github.com/bansallab/resp_contact`. Individual survey responses cannot be shared by the authors, but researchers can refer to `https://cmu-delphi.github.io/delphi-epidata/symptom-survey/data-access.html` if they would like to enter an agreement for data usage with CMU Delphi.

Acknowledgments

The authors thank the Carnegie Mellon University Delphi team for sharing the US COVID-19 Trends and Impact Survey results openly and freely and Casey Zipfel for sharing pandemic policy data.

References

1. Mossong J, Hens N, Jit M, Beutels P, Auranen K, Mikolajczyk R, et al. Social Contacts and Mixing Patterns Relevant to the Spread of Infectious Diseases. PLOS Medicine. 2008 Mar;5(3):e74.

2. Hoang T, Coletti P, Melegaro A, Wallinga J, Grijalva CG, Edmunds JW, et al. A Systematic Review of Social Contact Surveys to Inform Transmission Models of Close-contact Infections. Epidemiology. 2019 Sep;30(5):723–736.

3. Bansal S, Grenfell BT, Meyers LA. When Individual Behaviour Matters: Homogeneous and Network Models in Epidemiology. Journal of The Royal Society Interface. 2007;4:879–891.

4. Gostic KM, McGough L, Baskerville EB, Abbott S, Joshi K, Tedijanto C, et al. Practical Considerations for Measuring the Effective Reproductive Number, Rt. PLOS Computational Biology. 2020 Dec;16(12):e1008409.

5. Lloyd-Smith JO, Schreiber SJ, Kopp PE, Getz WM. Superspreading and the Effect of Individual Variation on Disease Emergence. Nature. 2005 Nov;438(7066):355–359.

6. Rohani P, Zhong X, King AA. Contact Network Structure Explains the Changing Epidemiology of Pertussis. Science. 2010 Nov;330(6006):982–985.

7. Mistry D, Litvinova M, Pastore y Piontti A, Chinazzi M, Fumanelli L, Gomes MFC, et al. Inferring High-Resolution Human Mixing Patterns for Disease Modeling. Nature Communications. 2021 Jan;12(1):323.

8. Kretzschmar ME, Rozhnova G, Bootsma MCJ, van Boven M, van de Wijgert JHHM, Bonten MJM. Impact of Delays on Effectiveness of Contact Tracing Strategies for COVID-19: A Modelling Study. The Lancet Public Health. 2020 Aug;5(8):e452–e459.

9. Aleta A, Martín-Corral D, Pastore y Piontti A, Ajelli M, Litvinova M, Chinazzi M, et al. Modelling the Impact of Testing, Contact Tracing and Household Quarantine on Second Waves of COVID-19. Nature Human Behaviour. 2020 Sep;4(9):964–971.

10. Overton CE, Stage HB, Ahmad S, Curran-Sebastian J, Dark P, Das R, et al. Using Statistics and Mathematical Modelling to Understand Infectious Disease Outbreaks: COVID-19 as an Example. Infectious Disease Modelling. 2020 Jan;5:409–441.

11. Gimma A, Munday JD, Wong KLM, Coletti P, van Zandvoort K, Prem K, et al. Changes in Social Contacts in England during the COVID-19 Pandemic between March 2020 and March 2021 as Measured by the CoMix Survey: A Repeated Cross-Sectional Study. PLOS Medicine. 2022 Mar;19(3):e1003907.

12. Coletti P, Wambua J, Gimma A, Willem L, Vercruysse S, Vanhoutte B, et al. CoMix: Comparing Mixing Patterns in the Belgian Population during and after Lockdown. Scientific Reports. 2020 Dec;10(1):21885.

13. Munday JD, Abbott S, Meakin S, Funk S. Evaluating the Use of Social Contact Data to Produce Age-Specific Short-Term Forecasts of SARS-CoV-2 Incidence in England. PLOS Computational Biology. 2023 Sep;19(9):e1011453.

14. Viboud C, Bjørnstad ON, Smith DL, Simonsen L, Miller MA, Grenfell BT. Synchrony, Waves, and Spatial Hierarchies in the Spread of Influenza. Science. 2006 Apr;312(5772):447–451.

15. Favier C, Schmit D, Müller-Graf CDM, Cazelles B, Degallier N, Mondet B, et al. Influence of Spatial Heterogeneity on an Emerging Infectious Disease: The Case of Dengue Epidemics. Proceedings of the Royal Society B: Biological Sciences. 2005 Jun;272(1568):1171–1177.

16. Susswein Z, Valdano E, Brett T, Rohani P, Colizza V, Bansal S. Ignoring Spatial Heterogeneity in Drivers of SARS-CoV-2 Transmission in the US Will Impede Sustained Elimination. medRxiv. 2021 Aug;.

17. Truelove SA, Graham M, Moss WJ, Metcalf CJE, Ferrari MJ, Lessler J. Characterizing the Impact of Spatial Clustering of Susceptibility for Measles Elimination. Vaccine. 2019 Jan;37(5):732–741.

18. Bharti N, Tatem AJ, Ferrari MJ, Grais RF, Djibo A, Grenfell BT. Explaining Seasonal Fluctuations of Measles in Niger Using Nighttime Lights Imagery. Science. 2011 Dec;334(6061):1424–1427.

19. Kummer AG, Zhang J, Jiang C, Litvinova M, Ventura PC, Garcia MA, et al. Evaluating Seasonal Variations in Human Contact Patterns and Their Impact on the Transmission of Respiratory Infectious Diseases. Infectious Diseases (except HIV/AIDS); 2022.

20. DeStefano F, Haber M, Currivan D, Farris T, Burrus B, Stone-Wiggins B, et al. Factors Associated with Social Contacts in Four Communities during the 2007–2008 Influenza Season. Epidemiology & Infection. 2011 Aug;139(8):1181–1190.

21. Zagheni E, Billari FC, Manfredi P, Melegaro A, Mossong J, Edmunds WJ. Using Time-Use Data to Parameterize Models for the Spread of Close-Contact Infectious Diseases. American Journal of Epidemiology. 2008 Nov;168(9):1082–1090.

22. Breen CF, Mahmud AS, Feehan DM. Novel Estimates Reveal Subnational Heterogeneities in Disease-Relevant Contact Patterns in the United States. PLOS Computational Biology. 2022 Dec;18(12):e1010742.

23. Taube JC, Susswein Z, Bansal S. Spatiotemporal Trends in Self-Reported Mask-Wearing Behavior in the United States: Analysis of a Large Cross-sectional Survey. JMIR Public Health and Surveillance. 2023 Mar;9(1):e42128.

24. Tiu A, Susswein Z, Merritt A, Bansal S. Characterizing the Spatiotemporal Heterogeneity of the COVID-19 Vaccination Landscape. American Journal of Epidemiology. 2022 Sep;191(10):1792–1802.

25. Dorélien AM, Ramen A, Swanson I, Hill R. Analyzing the Demographic, Spatial, and Temporal Factors Influencing Social Contact Patterns in U.S. and Implications for Infectious Disease Spread. BMC Infectious Diseases. 2021 Sep;21(1):1009.

26. Dorélien AM, Venkateswaran N, Deng J, Searle K, Enns E, Alarcon Espinoza G, et al. Quantifying Social Contact Patterns in Minnesota during Stay-at-Home Social Distancing Order. BMC Infectious Diseases. 2023 May;23(1):324.

27. Feehan DM, Mahmud AS. Quantifying Population Contact Patterns in the United States during the COVID-19 Pandemic. Nature Communications. 2021 Feb;12(1):893.

28. Nelson KN, Siegler AJ, Sullivan PS, Bradley H, Hall E, Luisi N, et al. Nationally Representative Social Contact Patterns among U.S. Adults, August 2020-April 2021. Epidemics. 2022 Sep;40:100605.

29. Klein B, LaRock T, McCabe S, Torres L, Friedland L, Kos M, et al. Characterizing Collective Physical Distancing in the U.S. during the First Nine Months of the COVID-19 Pandemic. PLOS Digital Health. 2024 Feb;3(2):e0000430.

30. Garnier R, Benetka JR, Kraemer J, Bansal S. Socioeconomic Disparities in Social Distancing During the COVID-19 Pandemic in the United States: Observational Study. Journal of Medical Internet Research. 2021 Jan;23(1):e24591.

31. Zang E, West J, Kim N, Pao C. U.S. Regional Differences in Physical Distancing: Evaluating Racial and Socioeconomic Divides during the COVID-19 Pandemic. PLOS ONE. 2021 Nov;16(11):e0259665.

32. Salomon JA, Reinhart A, Bilinski A, Chua EJ, La Motte-Kerr W, Rönn MM, et al. The US COVID-19 Trends and Impact Survey: Continuous Real-Time Measurement of COVID-19 Symptoms, Risks, Protective Behaviors, Testing, and Vaccination. Proceedings of the National Academy of Sciences. 2021 Dec;118(51):e2111454118.

33. Ingram DD, Franco SJ. 2013 NCHS Urban-Rural Classification Scheme for Counties. Vital and Health Statistics Series 2, Data Evaluation and Methods Research. 2014 Apr;(166):1–73.

34. Pedersen EJ, Miller DL, Simpson GL, Ross N. Hierarchical Generalized Additive Models in Ecology: An Introduction with Mgcv. PeerJ. 2019 May;7:e6876.

35. The New York Times. Coronavirus (Covid-19) Data in the United States; 2021. https://github.com/nytimes/covid-19-data.

36. Hale T, Angrist N, Goldszmidt R, Kira B, Petherick A, Phillips T, et al. A Global Panel Database of Pandemic Policies (Oxford COVID-19 Government Response Tracker). Nature Human Behaviour. 2021 Apr;5(4):529–538.

37. Zipfel C. The Interplay between Human Behavior and Infectious Disease Dynamics. Georgetown University; 2021.

38. Katz R, Toole K, Robertson H, Case A, Kerr J, Robinson-Marshall S, et al. Open Data for COVID-19 Policy Analysis and Mapping. Scientific Data. 2023 Jul;10(1):491.

39. Centers for Disease Control and Prevention. U.S. State and Territorial Gathering Bans: March 11, 2020-August 15, 2021 by County by Day | Data | Centers for Disease Control and Prevention;.

40. Centers for Disease Control and Prevention. U.S. State and Territorial Orders Closing and Reopening Bars Issued from March 11, 2020 through August 15, 2021 by County by Day | Data | Centers for Disease Control and Prevention;.

41. Centers for Disease Control and Prevention. U.S. State and Territorial Orders Closing and Reopening Restaurants Issued from March 11, 2020 through May 31, 2021 by County by Day | Data | Centers for Disease Control and Prevention;.

42. Centers for Disease Control and Prevention. U.S. State and Territorial Public Mask Mandates From April 10, 2020 through August 15, 2021 by County by Day | Data | Centers for Disease Control and Prevention;.

43. Centers for Disease Control and Prevention. U.S. State and Territorial Stay-At-Home Orders: March 15, 2020 – August 15, 2021 by County by Day | Data | Centers for Disease Control and Prevention;.

44. Safegraph. Social Distancing Metrics;. https://docs.safegraph.com/docs/social-distancing-metrics.

45. Crawford FW, Jones SA, Cartter M, Dean SG, Warren JL, Li ZR, et al. Impact of Close Interpersonal Contact on COVID-19 Incidence: Evidence from 1 Year of Mobile Device Data. Science Advances. 2022 Jan;8(1):eabi5499.

46. Tomori DV, Rübsamen N, Berger T, Scholz S, Walde J, Wittenberg I, et al. Individual social contact data and population mobility data as early markers of SARS-CoV-2 transmission dynamics during the first wave in Germanyâan analysis based on the COVIMOD study. BMC medicine. 2021;19:1–13.

47. Delussu F, Tizzoni M, Gauvin L. The Limits of Human Mobility Traces to Predict the Spread of COVID-19: A Transfer Entropy Approach. PNAS Nexus. 2023 Oct;2(10):pgad302.

48. Read JM, Eames KT, Edmunds WJ. Dynamic social networks and the implications for the spread of infectious disease. Journal of The Royal Society Interface. 2008;5(26):1001–1007.

49. Susswein Z, Rest EC, Bansal S. Disentangling the Rhythms of Human Activity in the Built Environment for Airborne Transmission Risk: An Analysis of Large-Scale Mobility Data. eLife. 2023 Apr;12:e80466.

50. CMMID COVID-19 working group, Jarvis CI, Van Zandvoort K, Gimma A, Prem K, Klepac P, et al. Quantifying the Impact of Physical Distance Measures on the Transmission of COVID-19 in the UK. BMC Medicine. 2020 Dec;18(1):124.

51. Pullano G, Alvarez-Zuzek LG, Colizza V, Bansal S. Characterizing US Spatial Connectivity: Implications for Geographical Disease Dynamics and Metapopulation Modeling. medRxiv; 2024.

52. Read JM, Lessler J, Riley S, Wang S, Tan LJ, Kwok KO, et al. Social Mixing Patterns in Rural and Urban Areas of Southern China. Proceedings of the Royal Society B: Biological Sciences. 2014 Jun;281(1785):20140268.

53. Kiti MC, Kinyanjui TM, Koech DC, Munywoki PK, Medley GF, Nokes DJ. Quantifying Age-Related Rates of Social Contact Using Diaries in a Rural Coastal Population of Kenya. PLOS ONE. 2014 Aug;9(8):e104786.

54. Kleynhans J, Tempia S, McMorrow ML, von Gottberg A, Martinson NA, Kahn K, et al. A Cross-Sectional Study Measuring Contact Patterns Using Diaries in an Urban and a Rural Community in South Africa, 2018. BMC Public Health. 2021 Jun;21(1):1055.

55. Mousa A, Winskill P, Watson OJ, Ratmann O, Monod M, Ajelli M, et al. Social Contact Patterns and Implications for Infectious Disease Transmission – a Systematic Review and Meta-Analysis of Contact Surveys. eLife. 2021 Nov;10:e70294.

Supplementary Materials

Additional CTIS details

The COVID-19 Trends and Impact Survey was created by researchers in the Delphi Group at Carnegie Mellon University and distributed via Facebook to active users 18 or older starting in April 2020. On a daily basis, a random state-stratified sample of Facebook users are invited to take the survey at the top of their news feed. These users will not be re-invited to take the survey for at least thirty days. The survey asks a broad range of questions related to COVID-19 symptoms and behaviors, with variations across each of the thirteen different waves spanning from April 2020 to June 2022. In this study, we make use of data from Wave 3 (May 21, 2020 - September 7, 2020), Wave 4 (September 8, 2020 - November 23, 2020), Wave 5 (November 24, 2020 - December 18, 2020), Wave 6 (December 19, 2020 - January 11, 2021), Wave 7 (January 12, 2021 - February 7, 2021), Wave 8 (February 8, 2021 - March 1, 2021), and Wave 10 (March 2, 2021 - May 19, 2021; Wave 9 was skipped for numbering purposes).

Weights were provided by Facebook for each response to adjust for non-response and coverage bias at the daily-state level [56]. Briefly, each weight describes the number of people represented by a respondent based on their age, gender, location, and date of response. These weights were calculated via a two-step process using inverse propensity score weighting based on respondents' demographics recorded in their Facebook user profiles to adjust the survey sample to reflect active Facebook users, followed by revisions of these weights using post-stratification so that the survey sample reflects the general population [32]. Because these weights were not at the same scale of our data analysis, we did not use them and instead performed raking to calculate our own weights as described below.

To address the lack of representation in this social media-administered survey, we calculated county-week weights for each observation using the `anesrake` package [58] and the US Census American Community Survey's 2021 data on county age and sex distributions. Age and sex distributions were based on each county's population over 18 to match the survey sample. We use three categories for age (18-24, 25-54, and 55+) and two categories for sex (ACS)/gender (CTIS) (male/man and female/woman). We assume that sex and gender are equivalent because the ACS doesn't collect gender identity information. Subsetting age further results in issues of nonconvergence. Including race or ethnicity was not possible in our raking approach as race/ethnicity data were only available for half the survey period and because convergence was not feasible with it. All analyses explicitly considering race/ethnicity are performed on data raked on race/ethnicity in addition to age and gender, and therefore are at a coarser spatial scale. We estimated mean contact for each county-week using a weighted mean of the responses with the calculated weights. We excluded observations with missing age or gender from the raking process and assigned equal weights to observations from county-weeks that did not converge. Demographic characteristics of respondents before and after weighting and compared to the Census are shown in Table S1.

As part of our data processing, we dropped responses missing fips codes, outside the 50 states and the District of Columbia, and from county-weeks with fewer than three responses.

We focused our analysis on non-household contacts; respondents were not explicitly asked about household contacts, and household contact distributions roughly aligned with those from the Census even without raking on this attribute (Figures S49 and S50). We note that non-household and household contacts were not highly correlated at the individual level (Pearson's correlation coefficient = 0.076).

Spatiotemporal contact estimation details

Generalized additive models were fit with a Gaussian family and identity link using the `bam` function with the `fREML` estimator from the `mgcv` version 1.8-39 R package [59]. To enforce smoother fits for all 50 states, the basis dimensions (k) were set at maximum 30 for the weekly smooth and maximum 15 for the county-level factor smooth with marginal penalty (m) 2 for the weekly smooth and 1 for the county factor smooth, and

a gamma value of 2 for each model. For DC, the weekly smooth had a maximum basis dimension of 10 with a penalized cubic regression spline. Diagnostic checks via `gam.check()` and `concurvity()` were completed to ensure that most p-values were not significant, k-indexes were close to 1, k' values were far from each edf, residuals were roughly normally distributed, and there was no heteroscedascity. Model adjusted-R^2s varied by state with a mean of 0.44 (Figure S26).

Baseline contact estimation details & diagnostics

We ran 3,080 linear regression models, one for each county with sufficient data. We show diagnostic plots for a random sample of counties demonstrating that our residuals did not display heteroscedascity or clear trends and are roughly normal (Figures S36 to S39). Across counties, the mean adjusted-R^2 was 0.93 and the mean GVIF was 6.00.

Contact by demographic or social classification model details

Age & gender

Using spatiotemporal GAMs, we estimated mean contact in four age groups for each county-week (18-54, 55-64, 65-74, 75+). We had to collapse age groups to have sufficient sample size, but note that contact rates among the 18-54 age group were quite similar prior to aggregation (Figure S48). This analysis was limited to counties with 5 or more responses in each age group for each of the 30 weeks from October 2020 through April 2021 (224 counties). For each age group separately, we estimated pandemic contact using the spatiotemporal GAMs and baseline contact using linear regression as described above. The same steps were followed for the two gender classes in the survey; there were 889 counties with sufficient sample size to estimate contact by gender. Given these sample size constraints, these results may not be representative of differences in contact patterns between age (and possibly gender) groups in the most rural US counties. This setup does allow us to compare age- and gender-specific regression coefficients describing the association between contact and disease incidence for each age/gender class.

Race/ethnicity

Using spatiotemporal GAMs, we estimated mean contact in five race/ethnicity categories (Asian, Black, Hispanic, other, and White) for each state-week. This analysis was limited to states with 10 or more responses in each racial/ethnic category for each of the 30 weeks from October 2020 through April 2021 (24 states) and was performed on the data that was reweighted by race/ethnicity, in addition to age and gender. Due to limited sample size, this analysis had to be performed at the state instead of the county level. For each racial/ethnic category separately, we estimated pandemic contact using the spatiotemporal GAMs and baseline contact using linear regression as described above with a couple exceptions. In the original GAMs we allowed for information sharing between counties within the same state; for these race/ethnicity-specific GAMs we instead allow for information sharing between states in the same census region of the US (West, Midwest, Northeast, South). For the linear regression, we predict contact using national incidence, state vaccination coverage, and state Oxford Stringency Index.

Setting

Using spatiotemporal GAMs, we estimated mean contact in four settings (work, social gatherings, shopping for essentials, and other) for each county-week. This analysis was limited to counties with 10 or more responses in each setting for each of the 30 weeks from October 2020 through April 2021. For each setting

separately, we estimated pandemic contact using the spatiotemporal GAMs and baseline contact using linear regression as described above.

Comparison to existing contact studies

We validated our findings with other work both before and during the pandemic, in Figures S1 to S19 below.

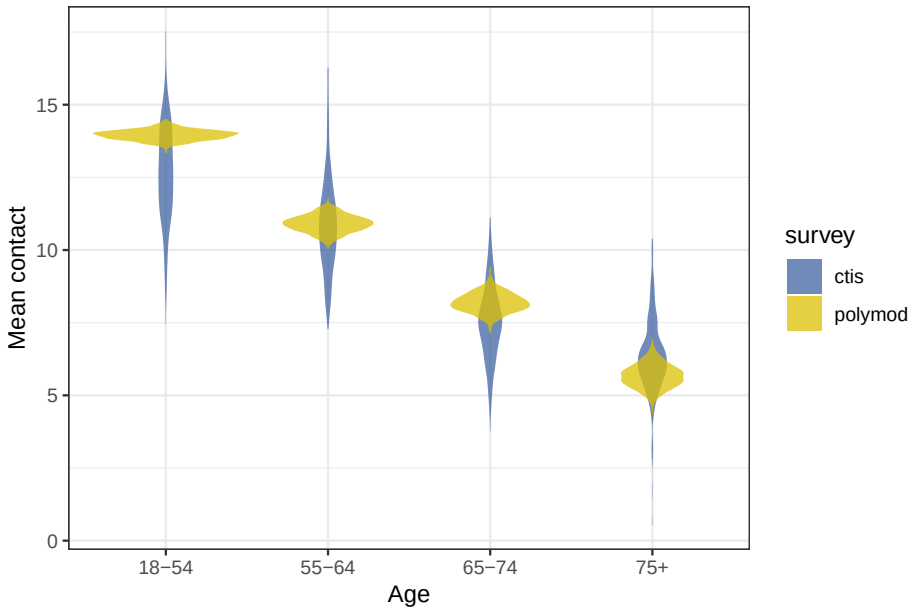

Figure S1. Comparison between our baseline contact estimates by age with those from the POLYMOD study [1]. Yellow violins are composed of bootstrapped means from 1,000 samples from the POLYMOD study (all responses equally weighted, truncated at 72 contacts, over all countries). Blue violins show the distribution of mean county-age group baseline estimates inferred from the CTIS.

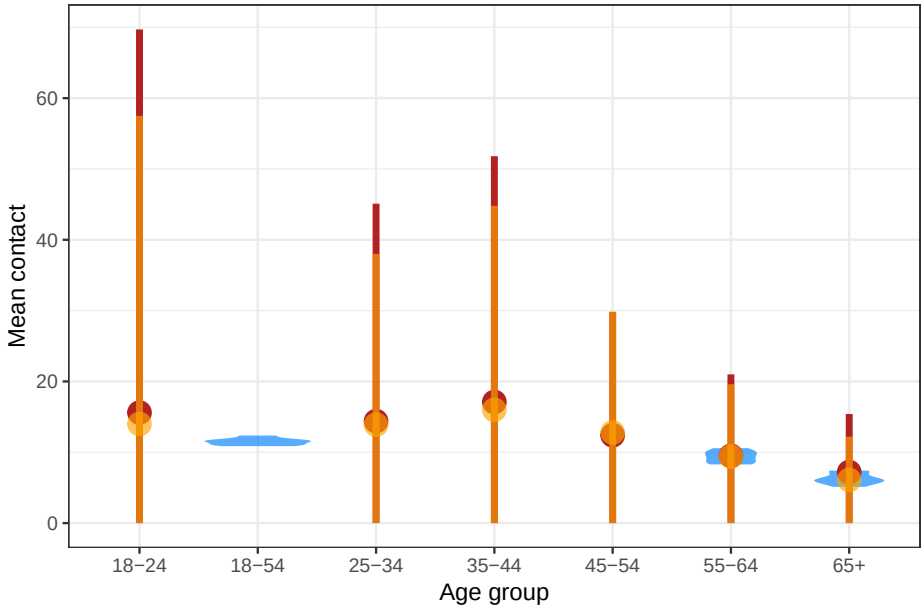

Figure S2. Comparison between our baseline contact estimates by age with those from [20]. Destefano and colleagues' [20] analyzed contact patterns across four counties in North Carolina, USA during the 2007-08 flu season, with 3,845 survey respondents. They measured both the mean number of speaking interactions (orange), defined as face to face conversations lasting at least one minute, and mean number of close proximity contacts (red), defined as within 6 feet for at least fifteen minutes. Point ranges represent one standard deviation above and below the mean (truncated at 0). Blue violins show the distribution of mean county-age group baseline estimates for seven North Carolina counties (those with sufficient group sample size) inferred from the CTIS.

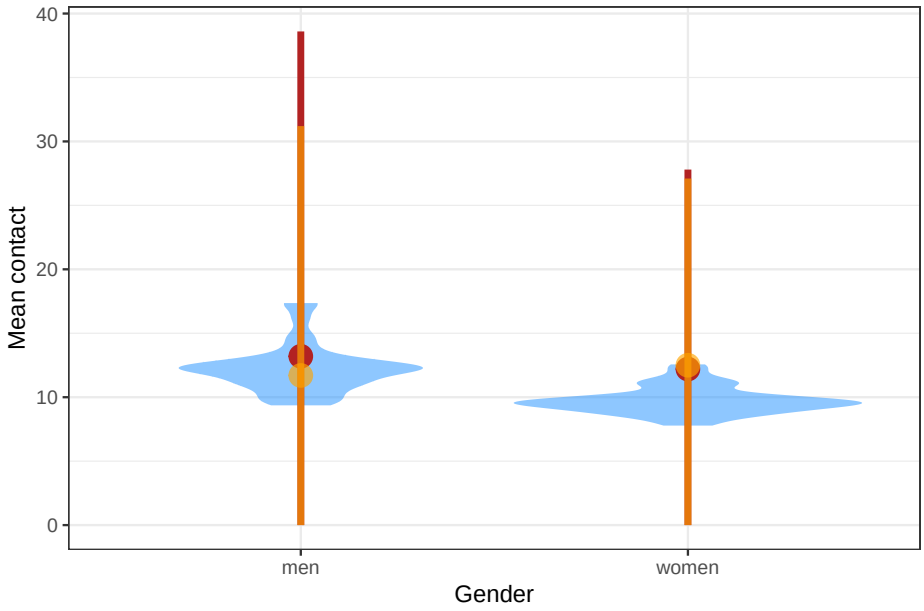

Figure S3. Comparison between our baseline contact estimates by gender with those from [20]. Destefano and colleagues' [20] analyzed contact patterns across four counties in North Carolina, USA during the 2007-08 flu season, with 3,845 survey respondents. They measured both the mean number of speaking interactions (orange), defined as face to face conversations lasting at least one minute, and mean number of close proximity contacts (red), defined as within 6 feet for at least fifteen minutes. Point ranges represent one standard deviation above and below the mean (truncated at 0). Blue violins show distribution of mean county-gender baseline estimates for 36 North Carolina counties (those with sufficient group sample size) inferred from the CTIS.

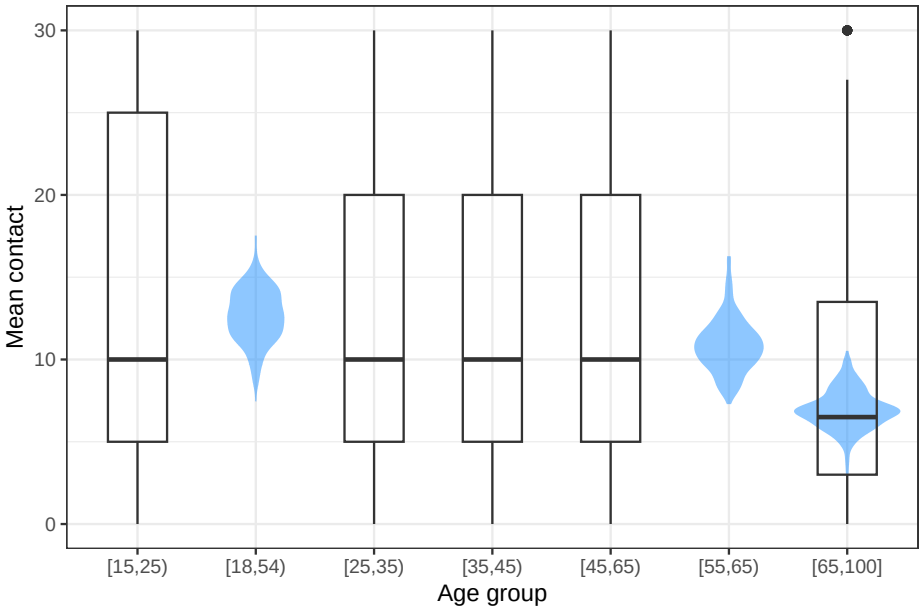

Figure S4. Comparison between our baseline contact estimates by age with those from [62]. Feehan and Cobb [62] conducted a national study of 3,076 Facebook users 15 years of age and older in the US before the pandemic (2015). They defined a contact as a face to face conversation containing at least three words. Boxplots were constructed using the raw data downloaded from `https://doi.org/10.7910/DVN/M74AJ4` `fb_ego.tab` file, where the center black line represents the median, the box summarizes the middle 50th percentile, the whiskers show the 1.5 times the interquartile range, and dots represent outliers. Blue violins show distribution of mean county-age group baseline estimates inferred from the CTIS.

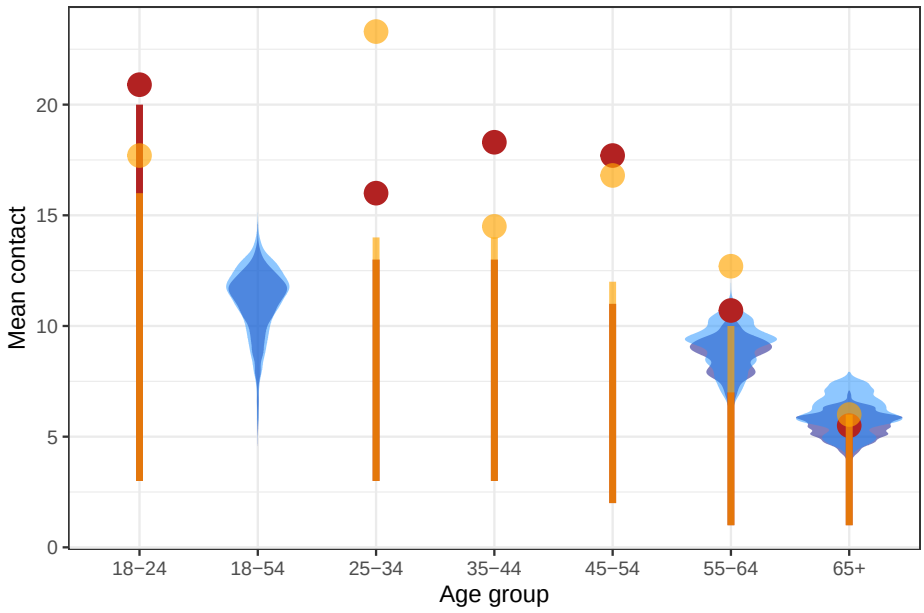

Figure S5. Comparison between our pandemic contact estimates by age with those from [28]. Nelson and colleagues' [28] conducted a nationally representative study of 3,112 individuals in the US during two periods, August - December 2020 (red) and March - April 2021 (orange). Contacts were defined as interactions within 6 feet involving the exchange of at least 3 words or involving physical touch. Red and orange points show the mean number of contacts for each time period, while ranges stretch from the 25th to 75th percentiles for each time period. Note that [28] truncated contacts at 50 per day and had smaller age group bins. Blue violins show the distribution of mean county-age group estimates from the CTIS: dark blue for August - December 2020 and light blue for March - April 2021 to match the time periods in Nelson et al., i.e. dark red and dark blue plots cover similar time periods and light orange and light blue plots cover similar time periods.

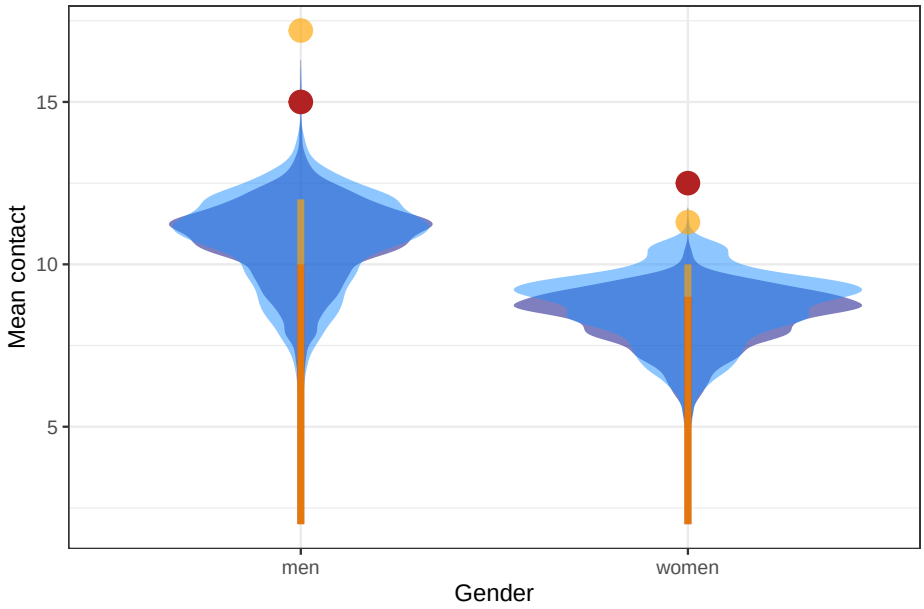

Figure S6. Comparison between our pandemic contact estimates by gender with those from [28]. Nelson and colleagues' [28] conducted a nationally representative study of 3,112 individuals in the US during two periods, August - December 2020 (red) and March - April 2021 (orange). Contacts were defined as interactions within 6 feet involving the exchange of at least 3 words or involving physical touch. Points show the mean number of contacts while ranges stretch from the 25th to 75th percentiles. Note that [28] truncated contacts at 50 per day. Blue violins show distribution of mean county-gender group estimates from the CTIS: dark blue for August - December 2020 and light blue for March - April 2021 to match the time periods in Nelson et al., i.e. dark red and dark blue plots cover similar time periods and light orange and light blue plots cover similar time periods.

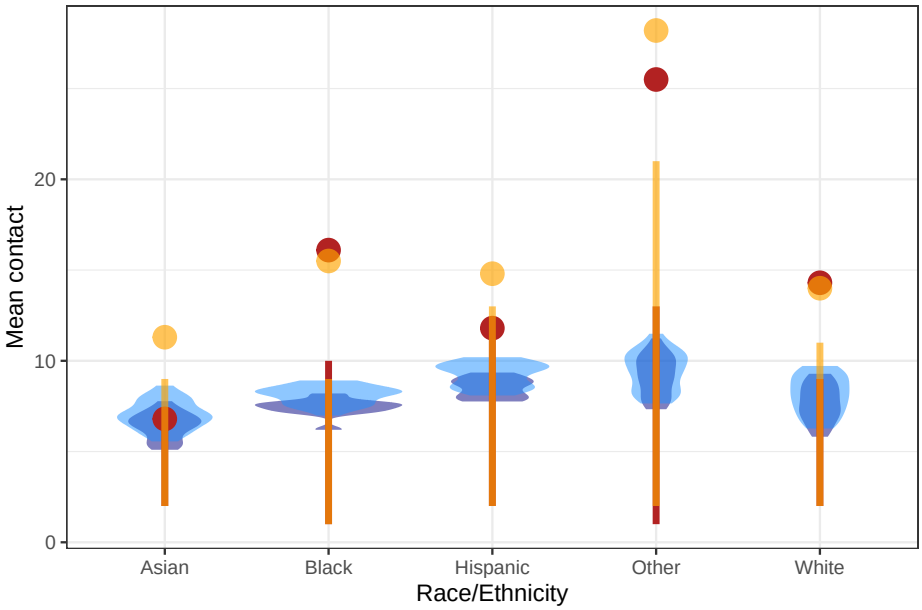

Figure S7. Comparison between our pandemic contact estimates by race/ethnicity with those from [28]. Nelson and colleagues' [28] conducted a nationally representative study of 3,112 individuals in the US during two periods, August - December 2020 (red) and March - April 2021 (orange). Contacts were defined as interactions within 6 feet involving the exchange of at least 3 words or involving physical touch. Points show the mean number of contacts while ranges stretch from the 25th to 75th percentiles. Note that [28] truncated contacts at 50 per day. Blue violins show distribution of mean state-race/ethnicity group estimates from the CTIS: dark blue for September - December 2020 and light blue for March - April 2021 to match the time periods in Nelson et al., i.e. dark red and dark blue plots cover similar time periods and light orange and light blue plots cover similar time periods.

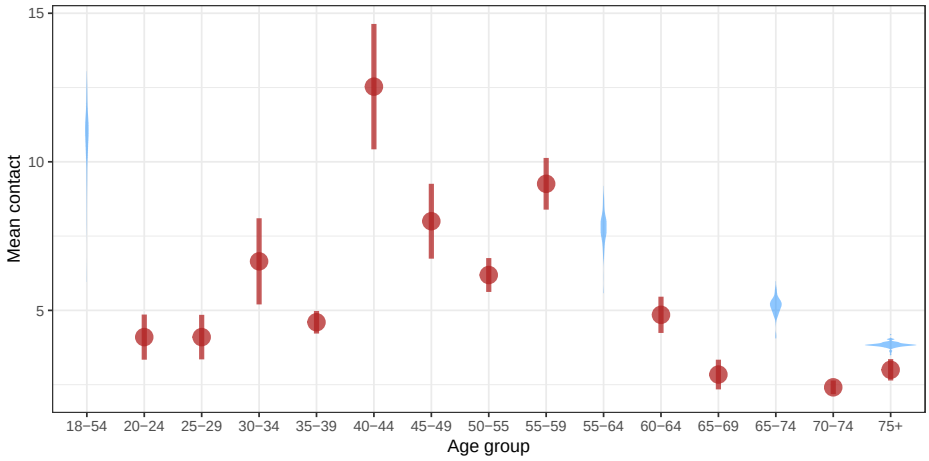

Figure S8. Comparison between our pandemic contact estimates by age with those from [26]. Dorelien and colleagues' [26] measured contact patterns in 2,083 children and adults in Minnesota, USA in April and May 2020. Contacts were defined as two-way conversations with 3+ words in the physical presence of another person or physical skin-to-skin contact. Red point ranges denote mean contact and one standard deviation above and below the mean from uncensored contact data. Blue violins show distribution of mean county-age group estimates for all 87 Minnesota counties from the CTIS for the first two weeks of May 2020 (these data are available in the CTIS but not as reliable).

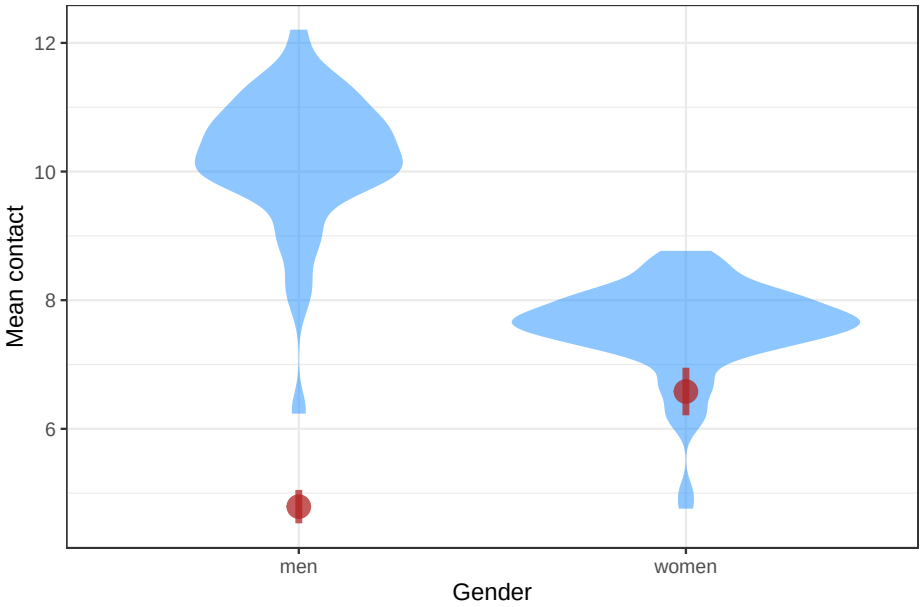

Figure S9. Comparison between our pandemic contact estimates by gender with those from [26]. Dorelien and colleagues' [26] measured contact patterns in 2,083 children and adults in Minnesota, USA in April and May 2020. Contacts were defined as two-way conversations with 3+ words in the physical presence of another person or physical skin-to-skin contact. Red point ranges denote mean contact and one standard deviation above and below the mean from uncensored contact data. Blue violins show distribution of mean county-gender group estimates for all 87 Minnesota counties from the CTIS for the first two weeks of May 2020 (these data are available in the CTIS but not as reliable).

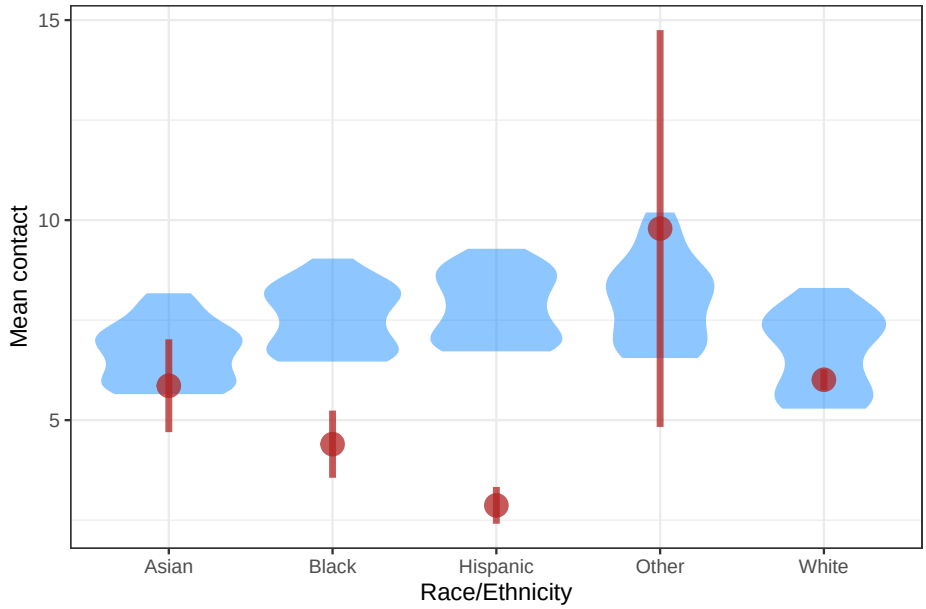

Figure S10. Comparison between our pandemic contact estimates by race/ethnicity with those from [26]. Dorelien and colleagues' [26] measured contact patterns in 2,083 children and adults in Minnesota, USA in April and May 2020. Contacts were defined as two-way conversations with 3+ words in the physical presence of another person or physical skin-to-skin contact. Red point ranges denote mean contact and one standard deviation above and below the mean from uncensored contact data. Blue violins show distribution of mean Minnesota race/ethnicity estimates from the CTIS for each week from September 2020 to April 2021 (a non-overlapping time period).

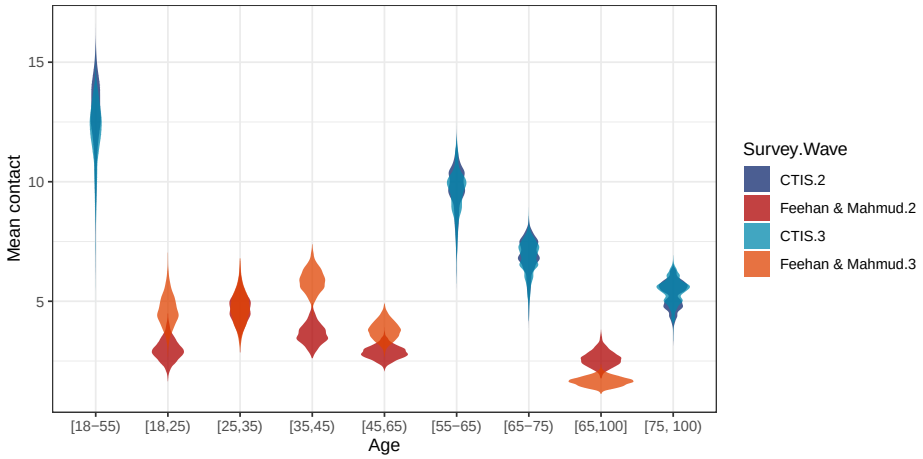

Figure S11. Comparison between our pandemic contact estimates by age with those from [27]. Feehan and Mahmud [27] conducted a nationally representative survey of contact patterns in the US including one week in June (Wave 2) and one week in September 2020 (Wave 3). Across the two waves, they had 2,641 respondents who reported fewer than 72 contacts. Red and orange violins show the bootstrapped mean contact for June and September 2020, respectively, using provided weights from [27]. (Note that we have imposed a truncation point on their data to match our analysis so the weights may no longer be accurate.) Blue and teal violins show the distribution of mean county-age group estimates from the CTIS for the same weeks in June and September, respectively.

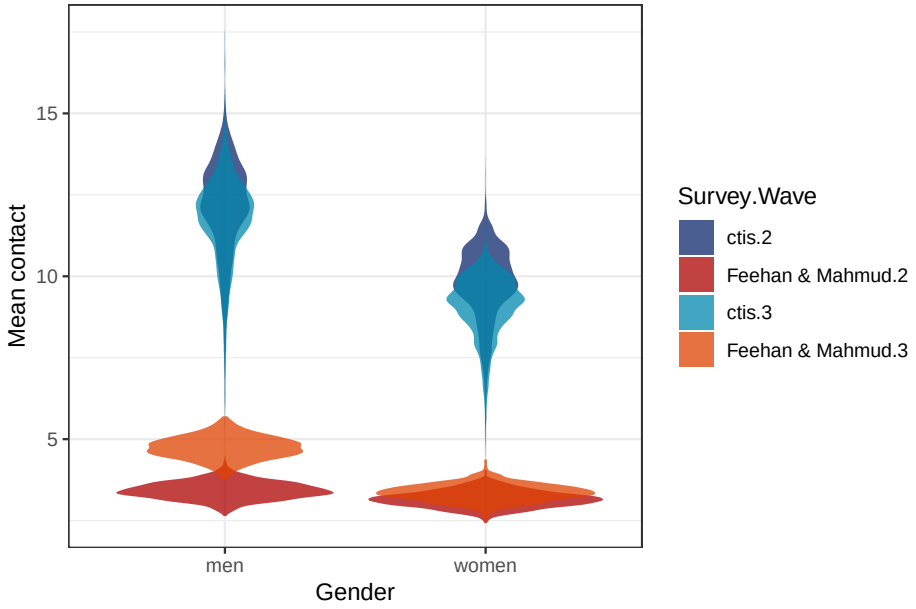

Figure S12. Comparison between our pandemic contact estimates by gender with those from [27]. Feehan and Mahmud [27] conducted a nationally representative survey of contact patterns in the US including one week in June (Wave 2) and one week in September 2020 (Wave 3). Across the two waves, they had 2,641 respondents who reported fewer than 72 contacts. Red and orange violins show the bootstrapped mean contact for June and September 2020, respectively, using provided weights from [27]. (Note that we have imposed a truncation point on their data to match our analysis so the weights may no longer be accurate.) Blue and teal violins show the distribution of mean county-gender estimates from the CTIS for same weeks in June and September, respectively.

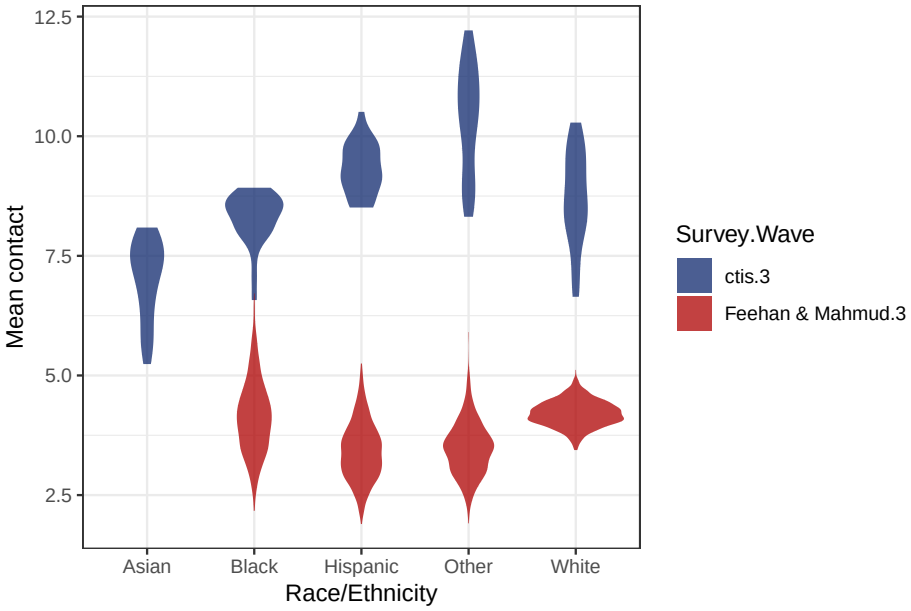

Figure S13. Comparison between our pandemic contact estimates by race/ethnicity with those from [27]. Feehan and Mahmud [27] conducted a nationally representative survey of contact patterns in the US including one week in September 2020 (Wave 3). In this wave, they had 1,514 respondents who reported fewer than 72 contacts. Red violins show the bootstrapped mean contact for September 2020, using provided weights from [27]. (Note that we have imposed a truncation point on their data to match our analysis so the weights may no longer be accurate.) Blue violins show distribution of mean state-race/ethnicity estimates from the CTIS for the same week in September 2020.

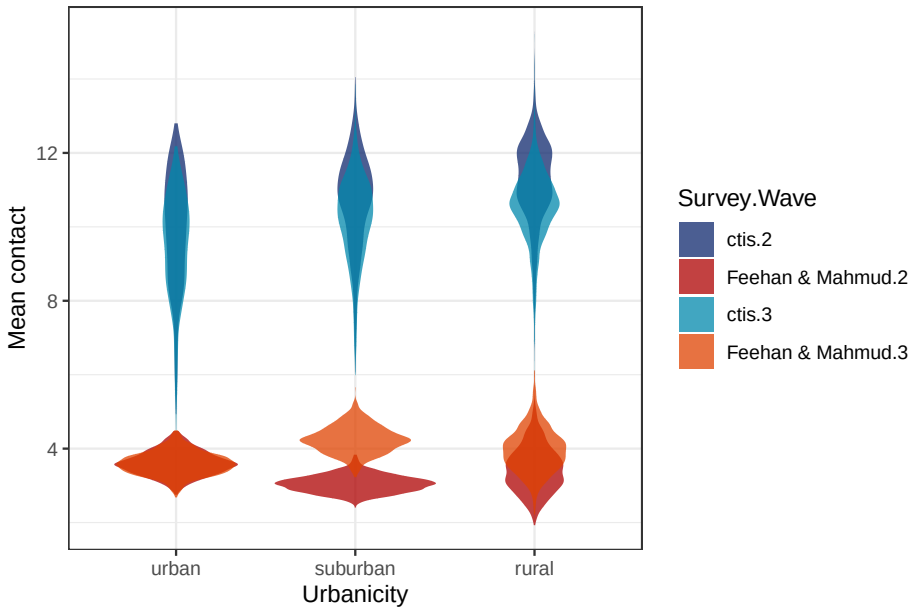

Figure S14. Comparison between our pandemic contact estimates by urbanicity with those from [27]. Feehan and Mahmud [27] conducted a nationally representative survey of contact patterns in the US including one week in June (Wave 2) and one week in September 2020 (Wave 3). Across the two waves, they had 2,641 respondents who reported fewer than 72 contacts. Respondents were classified as living in urban, suburban, or rural areas. Red and orange violins show the bootstrapped mean contact for June and September 2020, respectively, using provided weights from [27]. (Note that we have imposed a truncation point on their data to match our analysis so the weights may no longer be accurate.) Blue and teal violins show the distribution of mean county estimates from the CTIS for same weeks in June and September, respectively. CTIS data are at the county level; therefore, in this figure counties in NCHS classes 1 and 2 have been designated as urban, 3 and 4 as suburban, and 5 and 6 as rural for visualization purposes.

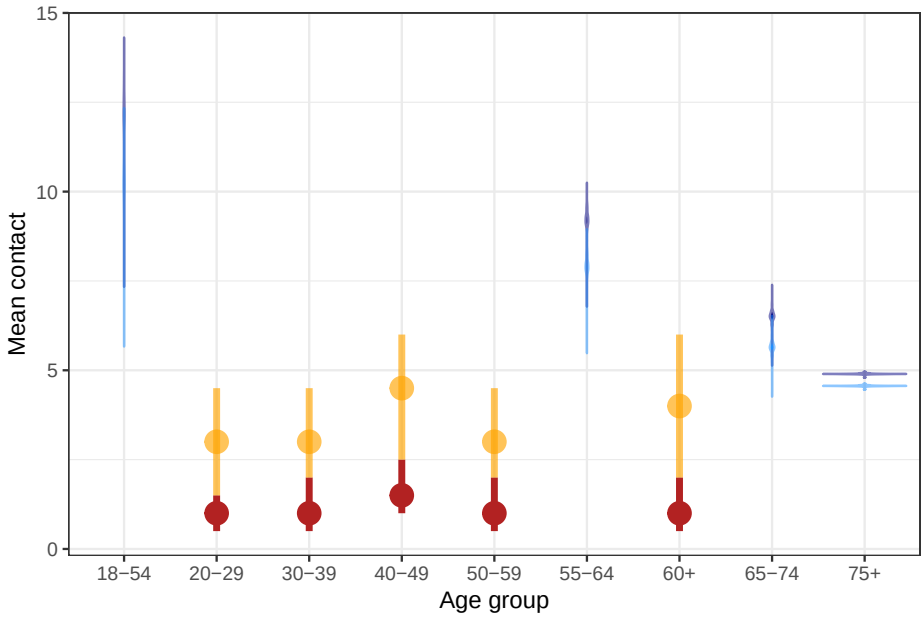

Figure S15. Comparison between our pandemic contact estimates by age with those from [66]. Kiti and colleagues' surveyed contact patterns across 647 employees of five private companies based in Georgia, USA over two days in April - June 2020 and November 2020 - January 2021. Contacts were categorized as interactions within 6 feet for less than 20 seconds, conversational contacts, or physical contacts, and included contacts in the home. Red and orange point ranges show the means and interquartile ranges of contact divided by two (to represent one day's worth of contacts) for April - June 2020 and November 2020 - January 2021 periods, respectively. Blue and navy violins show the distribution of mean county-age estimates for 158 counties in Georgia from the CTIS for the same time periods, respectively.

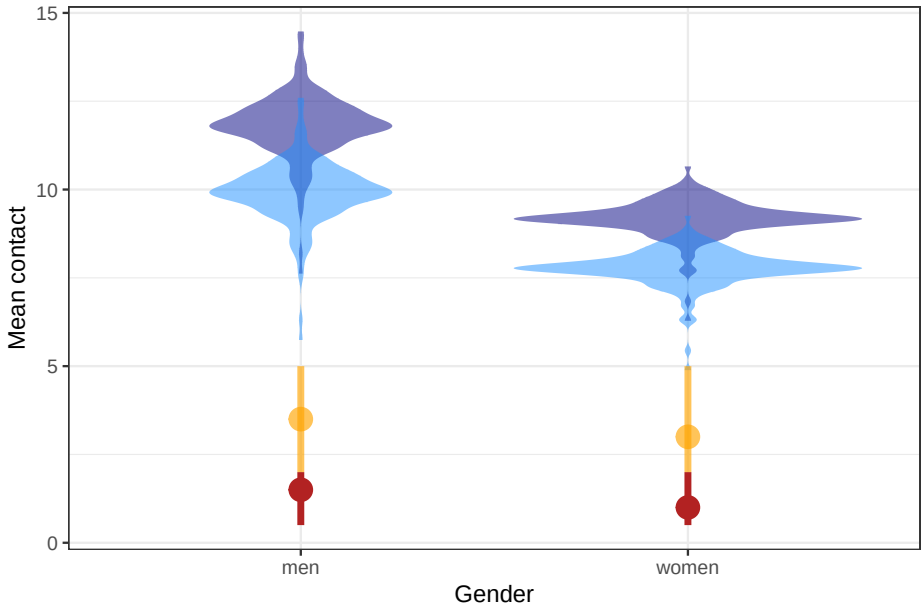

Figure S16. Comparison between our pandemic contact estimates by gender with those from [66]. Kiti and colleagues' surveyed contact patterns across 647 employees of five private companies based in Georgia, USA over two days in April - June 2020 and November 2020 - January 2021. Contacts were categorized as interactions within 6 feet for less than 20 seconds, conversational contacts, or physical contacts, and included contacts in the home. Red and orange point ranges show the means and interquartile ranges of contact divided by two (to represent one day's worth of contacts) for April - June 2020 and November 2020 - January 2021 periods, respectively. Blue and navy violins show the distribution of mean county-gender estimates for 158 counties in Georgia from the CTIS for the same time periods, respectively.

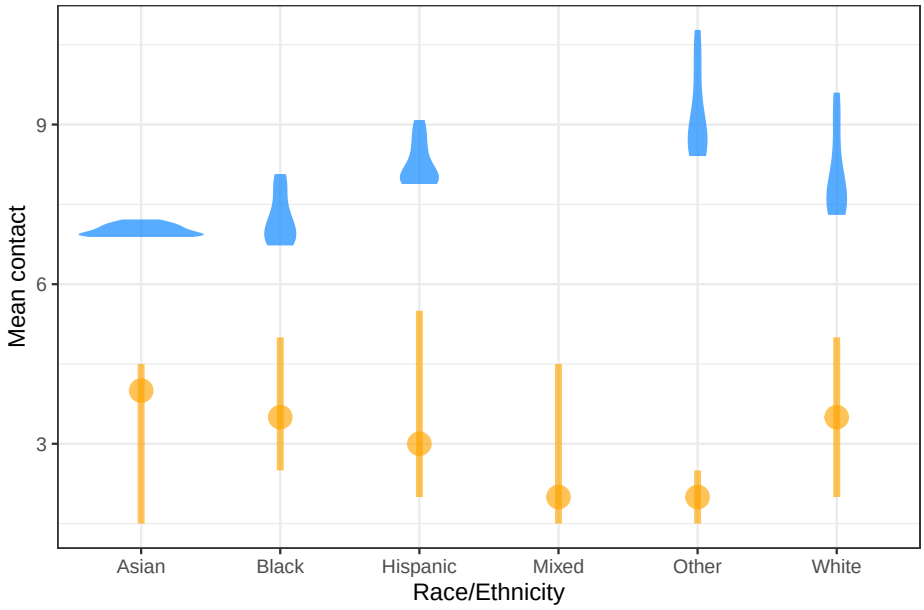

Figure S17. Comparison between our pandemic contact estimates by race/ethnicity with those from [66]. Kiti and colleagues' surveyed contact patterns across 647 employees of five private companies based in Georgia, USA over two days in November 2020 - January 2021. Contacts were categorized as interactions within 6 feet for less than 20 seconds, conversational contacts, or physical contacts, and included contacts in the home. Orange point ranges show the means and interquartile ranges of contact divided by two (to represent one day's worth of contacts) for November 2020 - January 2021 periods. Blue violins show the distribution of mean state-race/ethnicity estimates for Georgia from the CTIS for each week in the same time period.

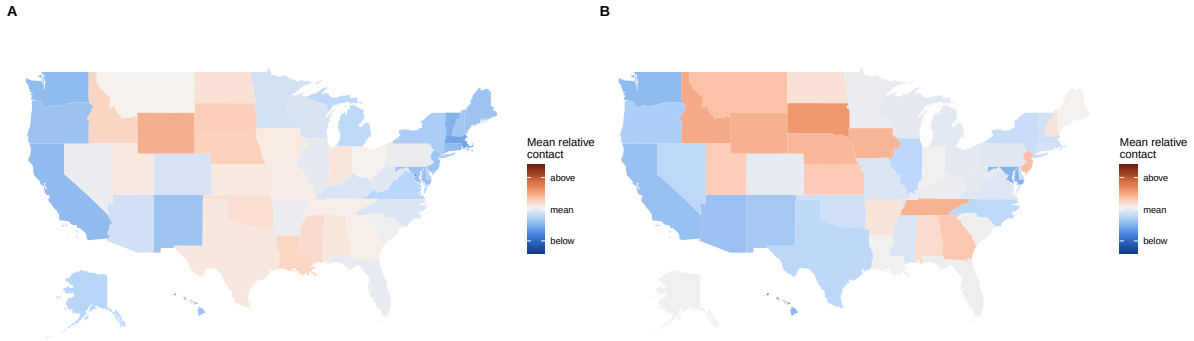

Figure S18. Comparison between (A) our findings and (B) Breen et al. [22] at the state level.

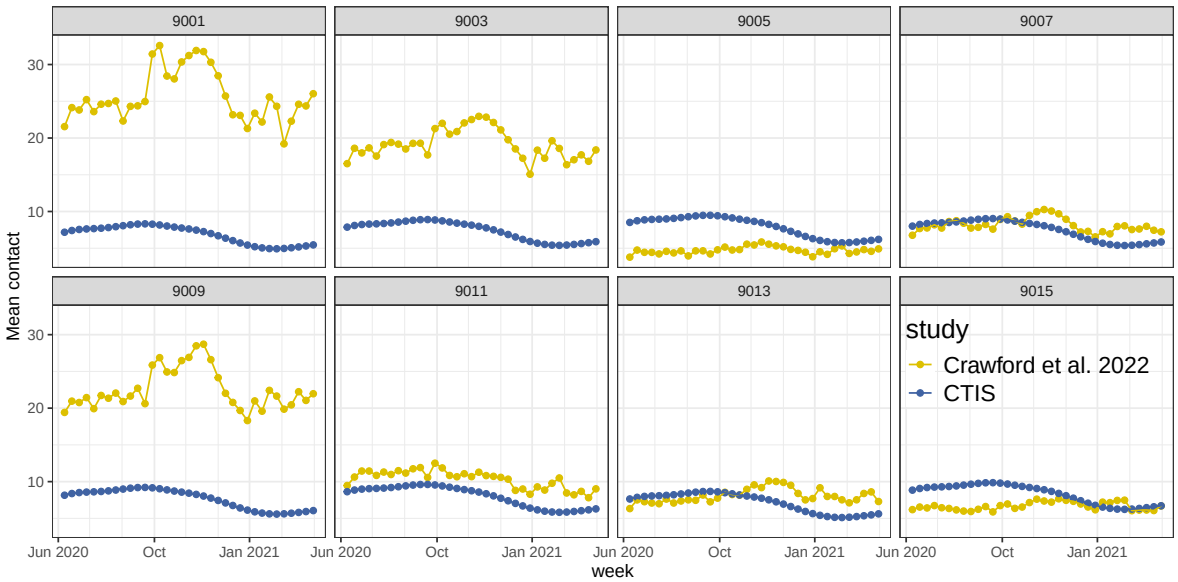

Figure S19. Comparison between our findings and those from [45]. [45] use mobile device geolocation data in Connecticut to estimate co-location within 2 meters. Here, we aggregate their town level estimates to the county level for comparison using an unweighted mean. [45] yields larger contact estimates than the CTIS, likely due to recall bias in the CTIS, no duration minimum for contact in [45], and the potential for double counting contacts with the same person in [45].

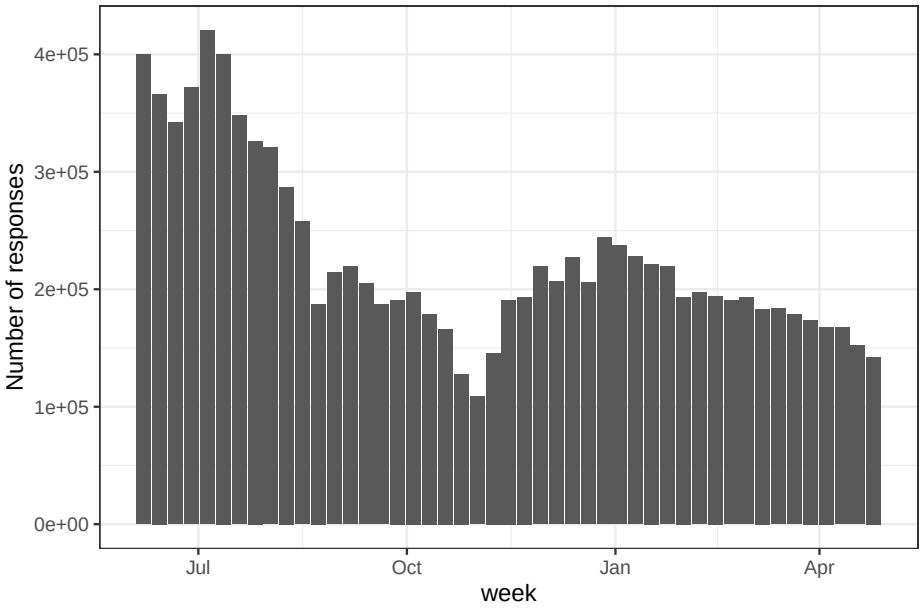

Figure S20. Weekly valid responses to the CTIS over the study period from June 2020 to April 2021.

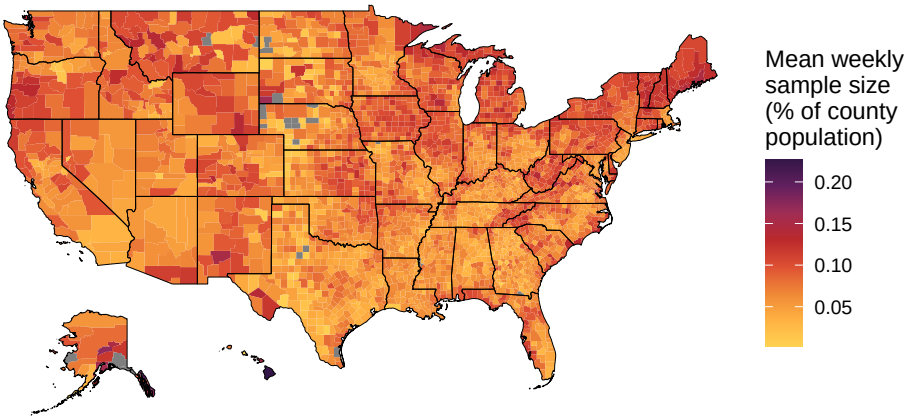

Figure S21. Mean number of weekly responses per county as a percentage of the county's total population.

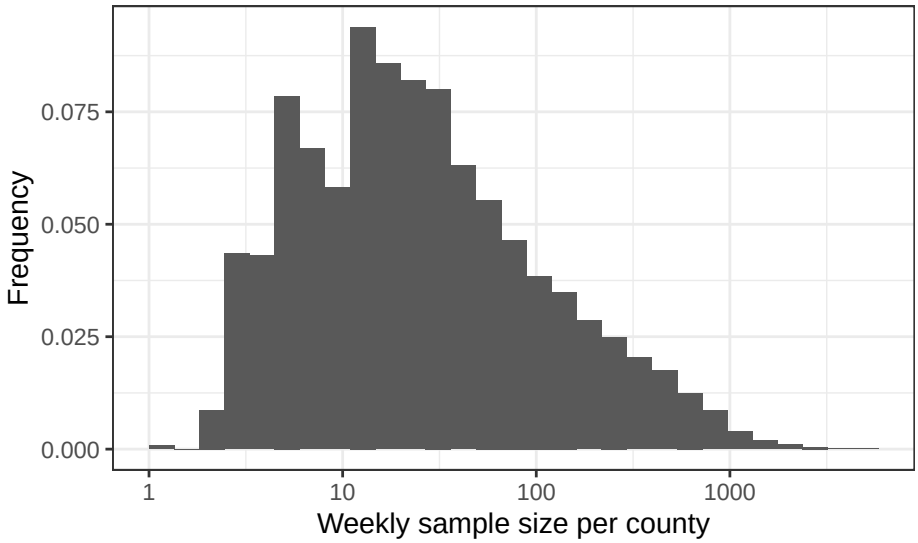

Figure S22. Weekly sample size by county. Note that the x-axis is on a log10 scale.

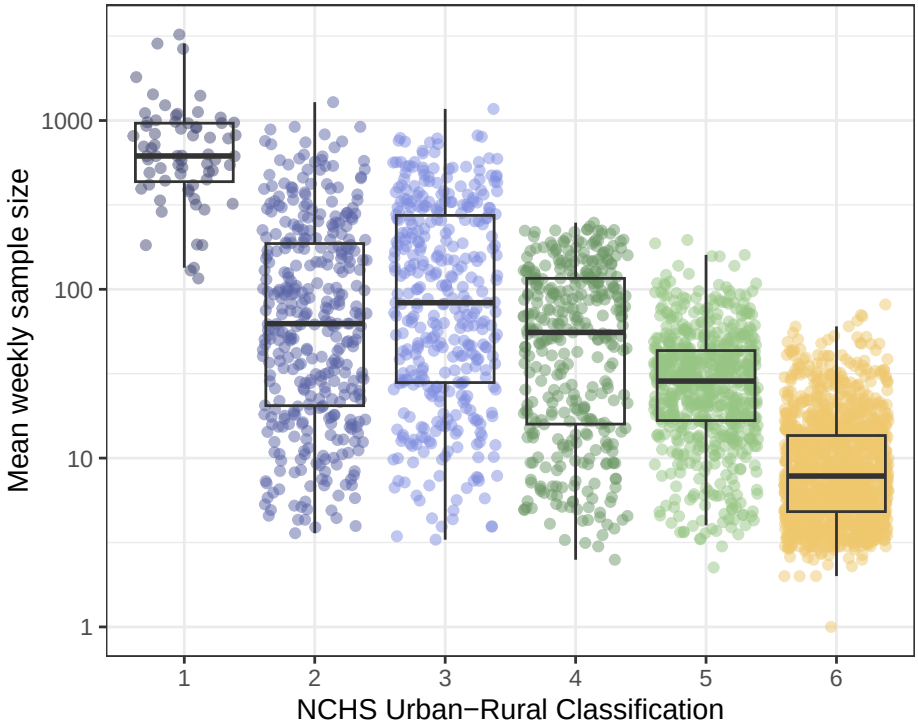

Figure S23. Weekly sample size by urban-rural designation. 1 represents the most urban and 6 the most rural. Note that the y-axis is on a log10 scale.

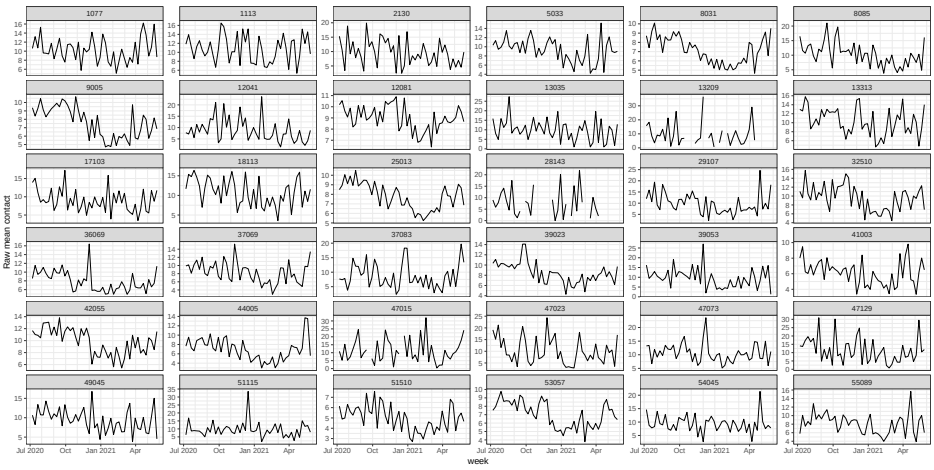

Figure S24. Example of raw contact time series. Estimates are very noisy before smoothing but show trend of decreased contact in winter 2020/2021.

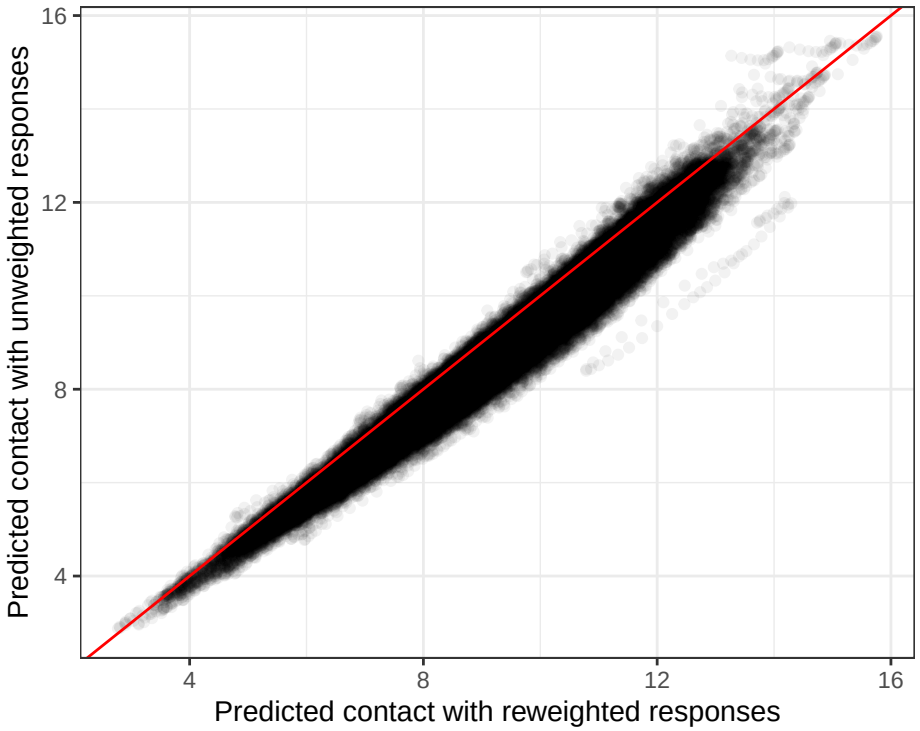

Figure S25. Comparison of modeled contact from GAMs run on reweighted (post-raking) versus unweighted data. Contact estimates are slightly higher after reweighting. This finding aligns with our expectation about survey sampling biases: we expect that the survey will disproportionately capture more COVID-19 cautious people with fewer contacts.

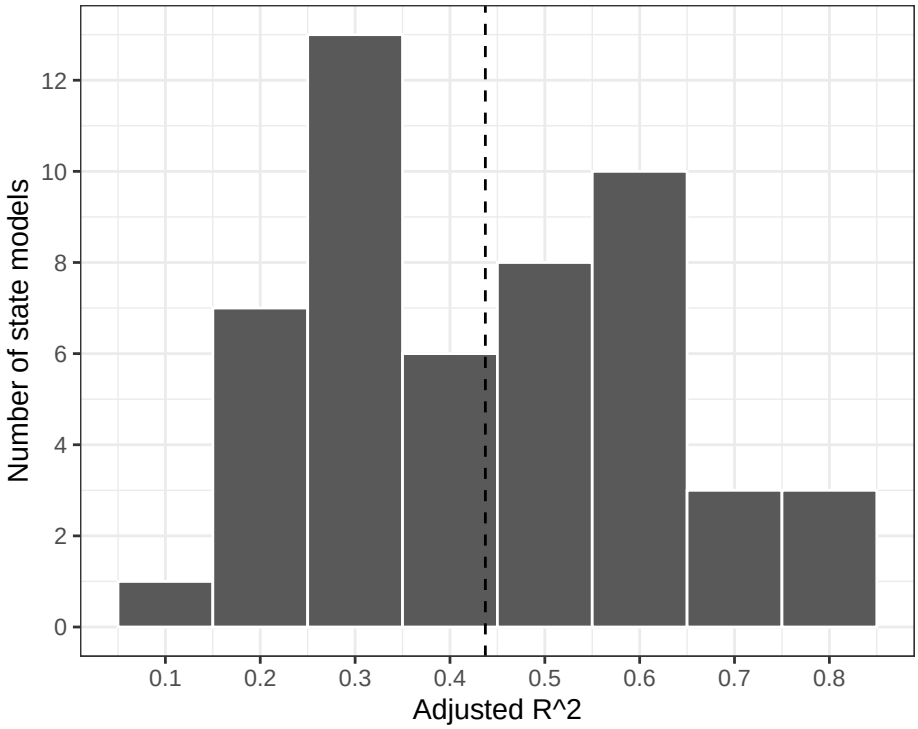

Figure S26. Distribution of adjusted R^2 values across state GAMs. Dashed line represents the mean adjusted-R^2 across states.

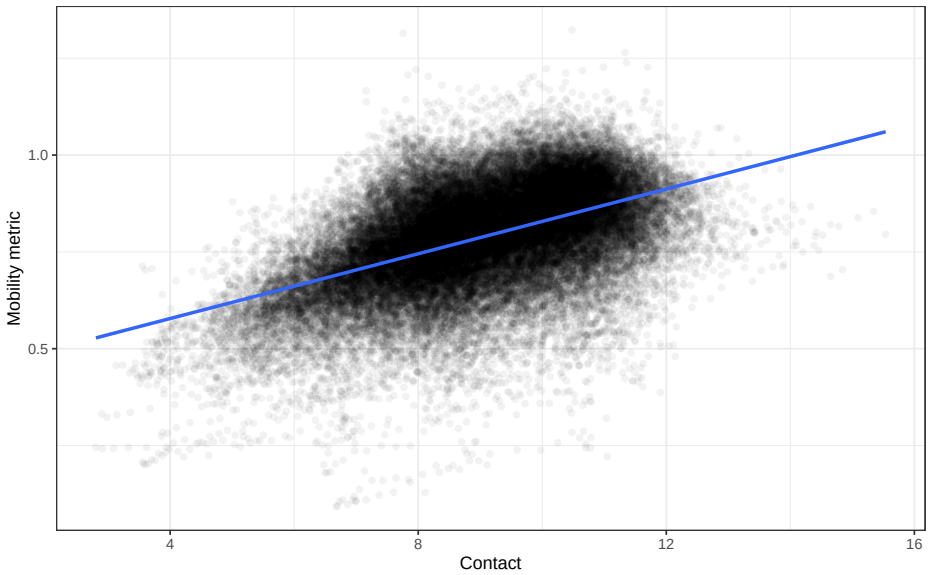

Figure S27. Mobility and contact are highly correlated. Data from September - December 2020. Mobility metric is the ratio of weekly 2019 to 2020 Safegraph visitor counts for each county.

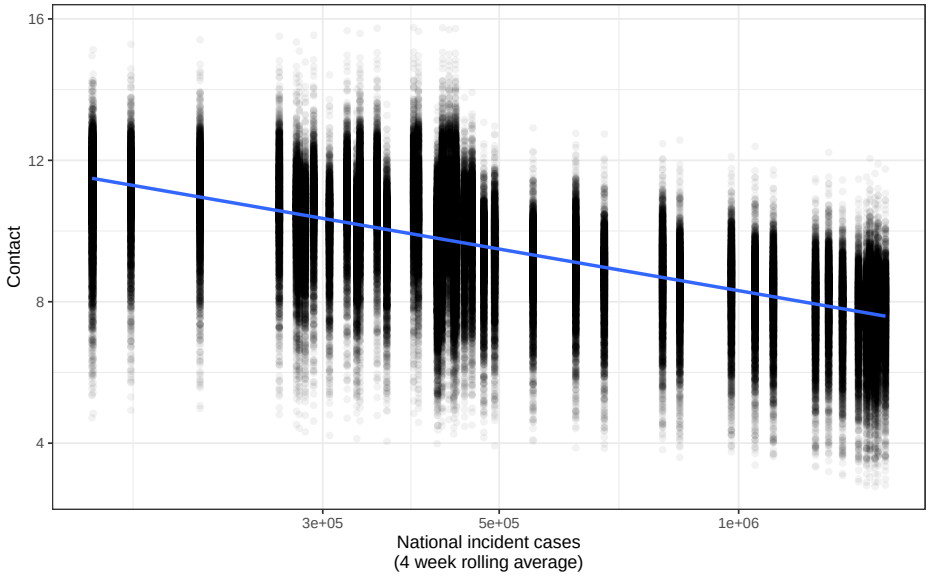

Figure S28. National incidence and contact are correlated. Data from June 2020 - April 2021. National incidence is the right-aligned 4 week rolling average.

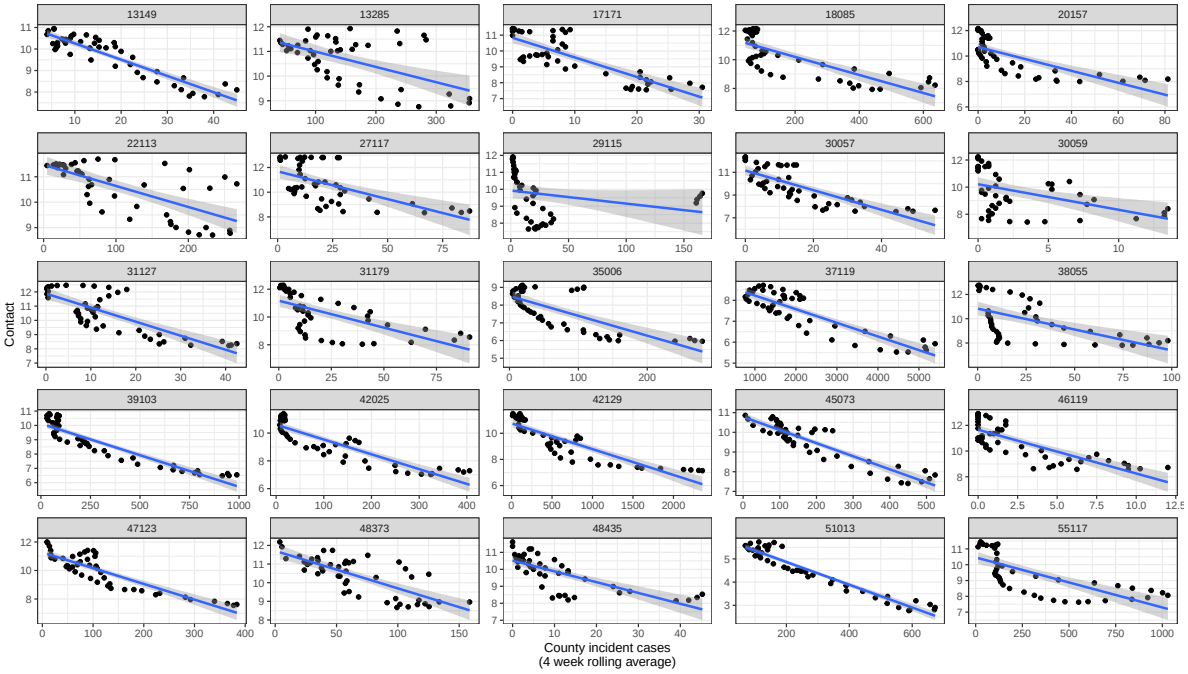

Figure S29. County incidence and contact are correlated. Data from June 2020 - April 2021. County incidence is the right-aligned 4 week rolling average.

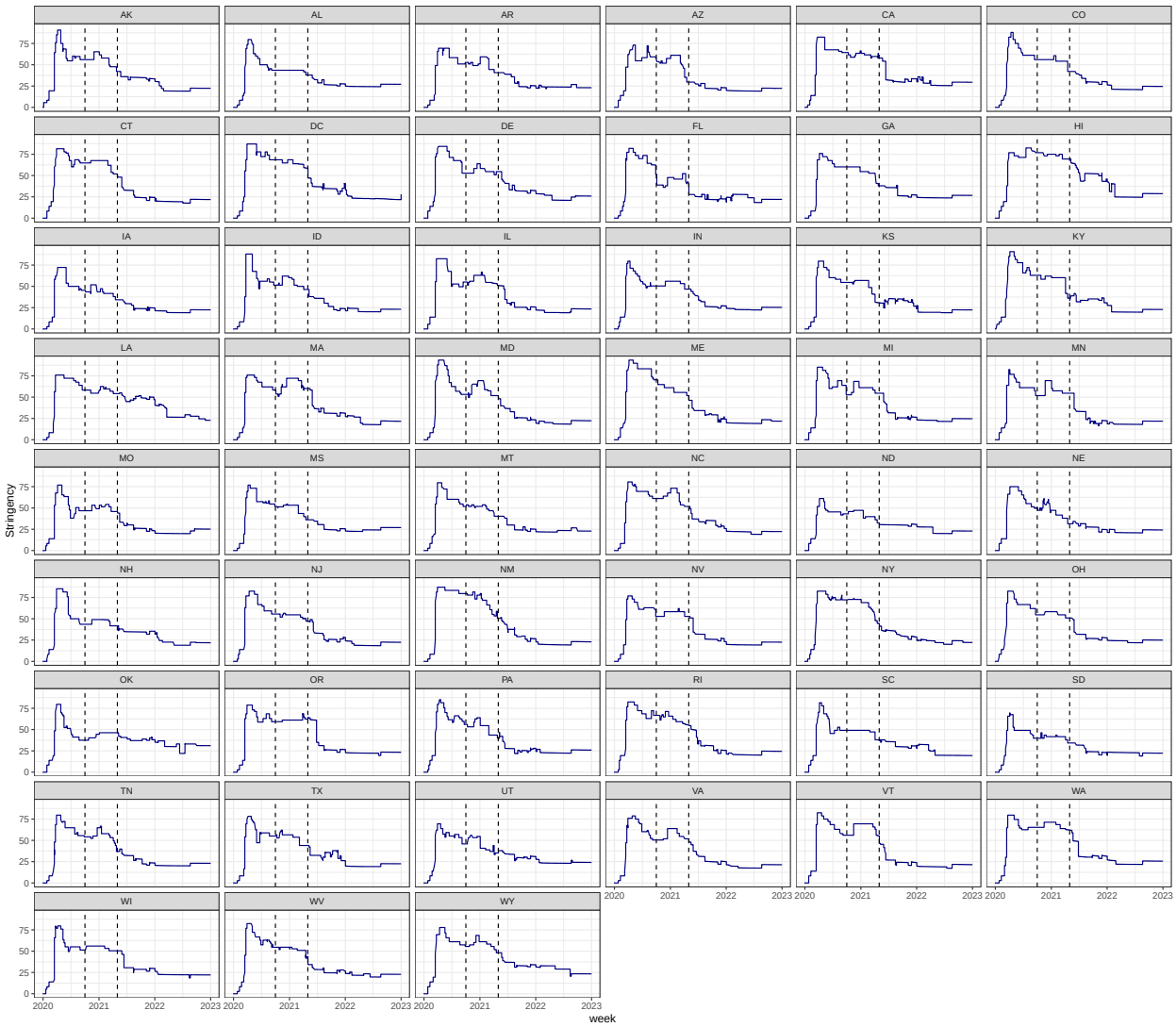

Figure S30. State stringency indices over time from [36]. Dashed lines denote the beginning and end of our baseline analysis study period.

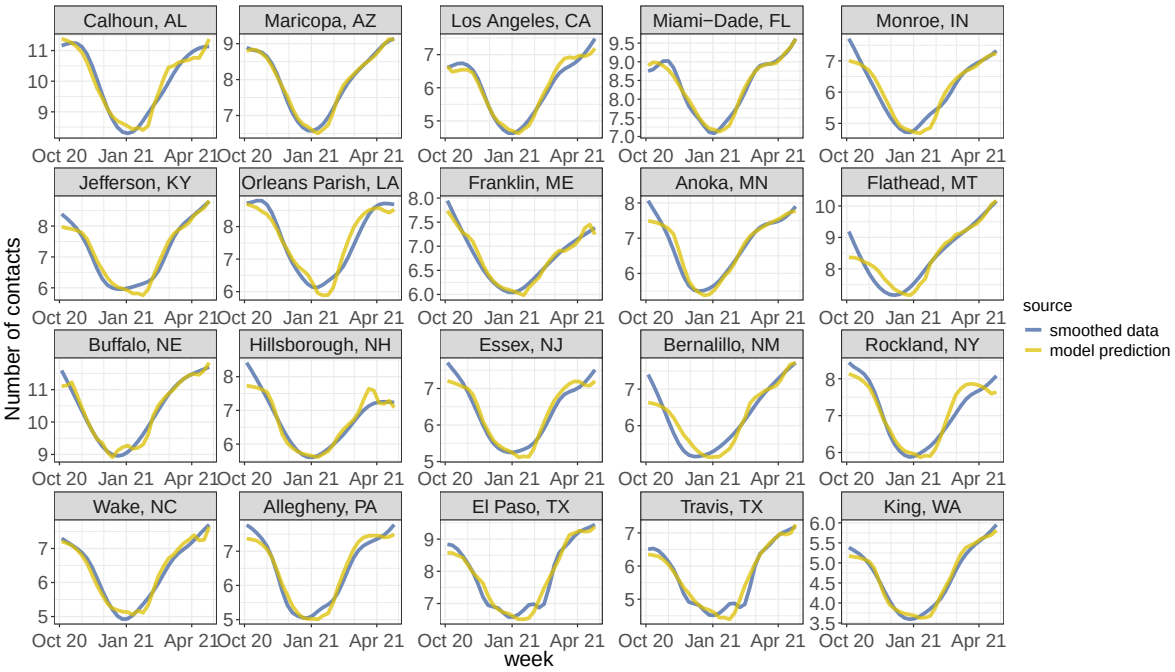

Figure S31. Smoothed contact data versus linear combination of incidence, policy, and vaccination terms in regression shows good fit between fluctuations in disease and contact.

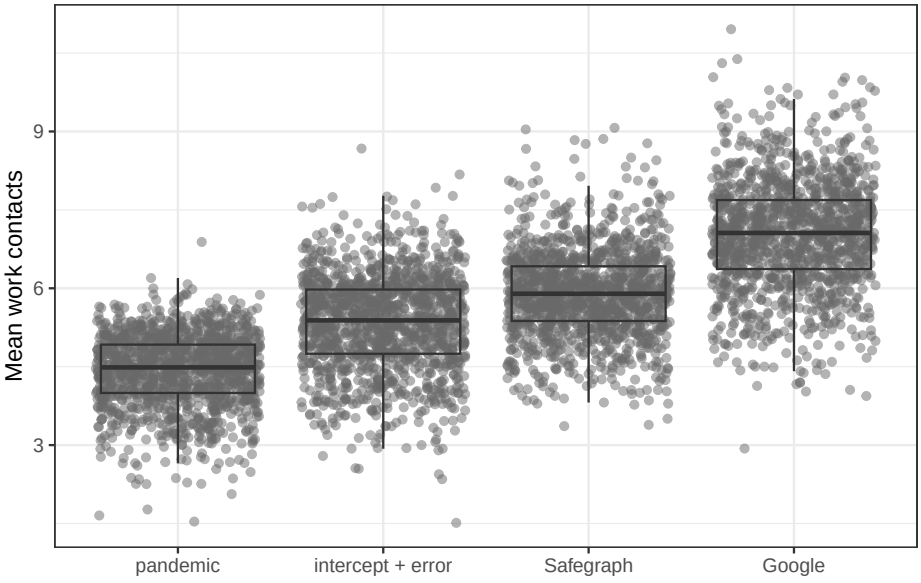

Figure S32. Using Google work-specific mobility data [70] to infer baseline work contacts yields higher estimates than Safegraph mobility data aggregated across all settings. Each point represents a county.

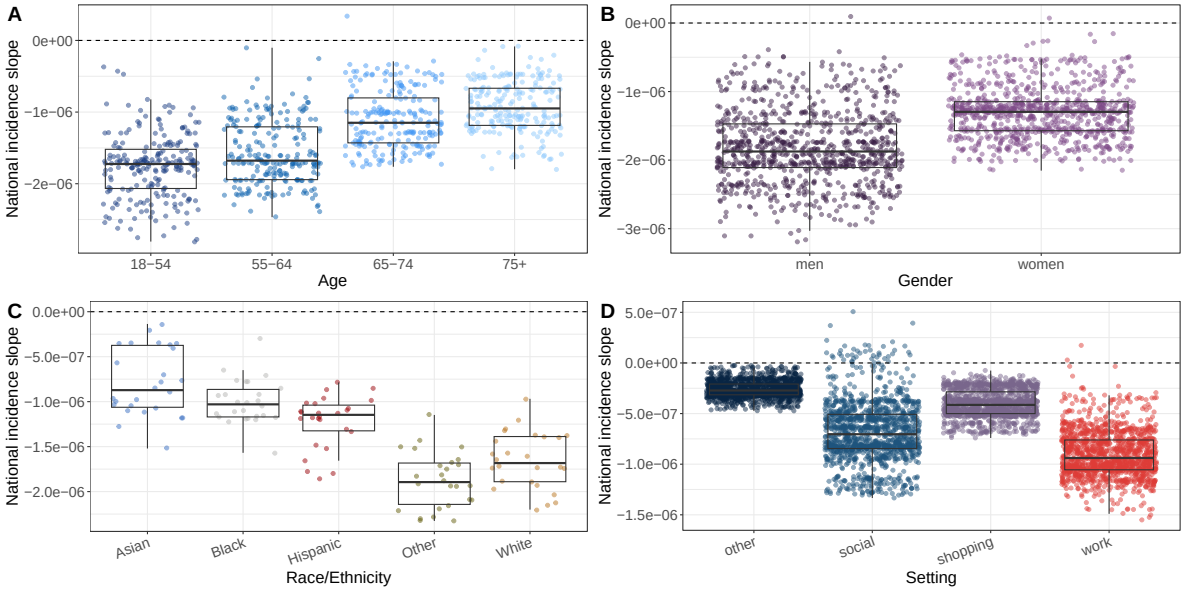

Figure S33. National disease incidence regression coefficient by age, gender, race/ethnicity, and setting. More negative coefficients indicate a stronger negative relationship between national incidence and non-household contacts, calculated during the baseline regression.

Figure S34. Fitted contact values by month. (A) June 2020 through (K) April 2021. While the mean changes, the spatial heterogeneity is relatively consistent.

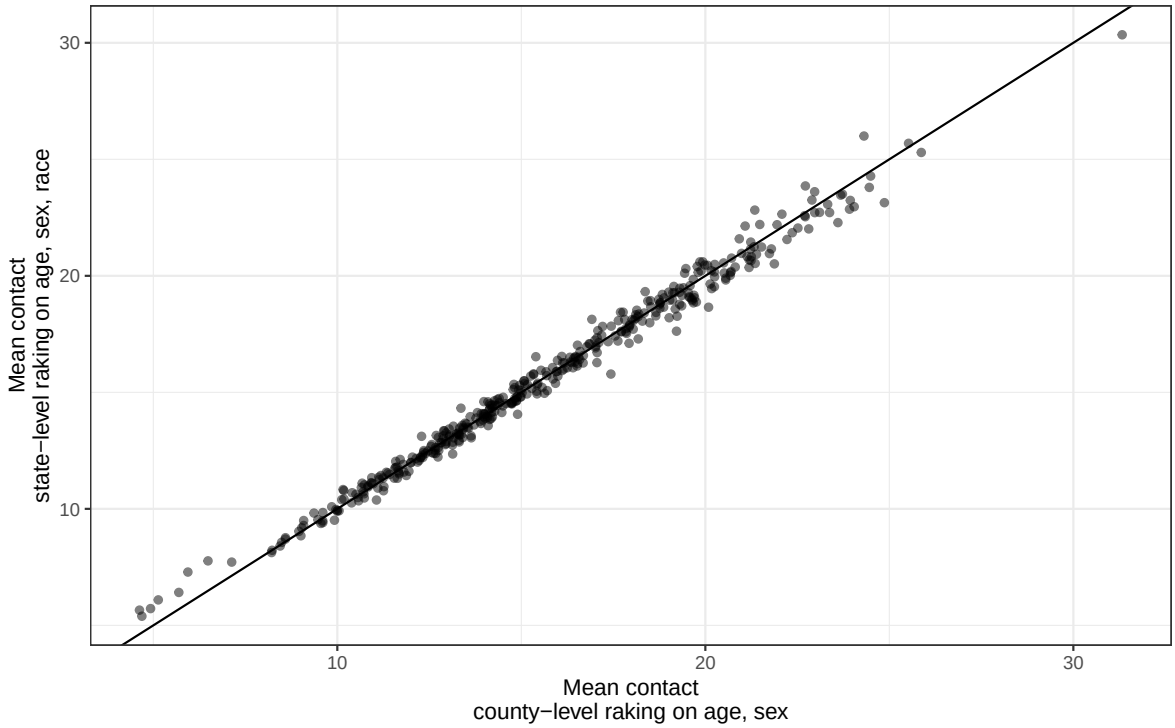

Figure S35. Raw pandemic contact estimates are minimally affected by raking on race in addition to age and gender. X-axis value is generated by raking at the county-level on age and gender and aggregating estimates to the state-month level. Y-axis value is generated by raking at the state-level on age, gender, and race and aggregating estimates to the monthly level.

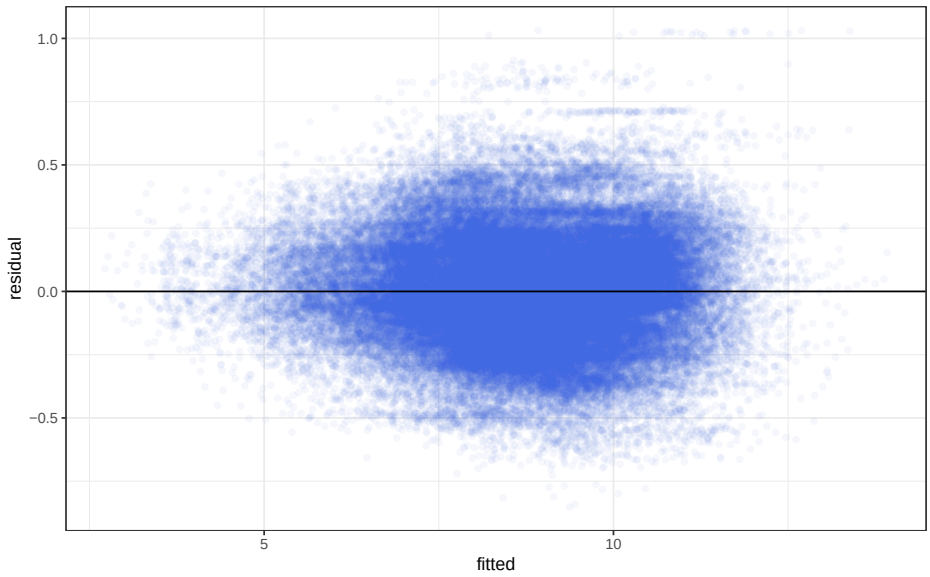

Figure S36. Residuals versus fitted values across all counties indicate no clear trends nor fanning/heteroscedascity.

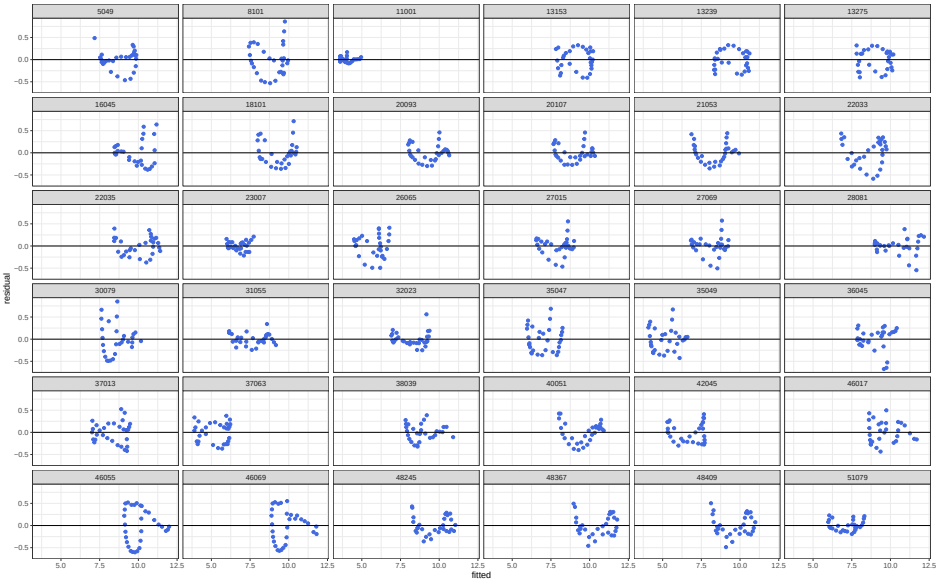

Figure S37. Residuals versus fitted values for a sample of random counties.

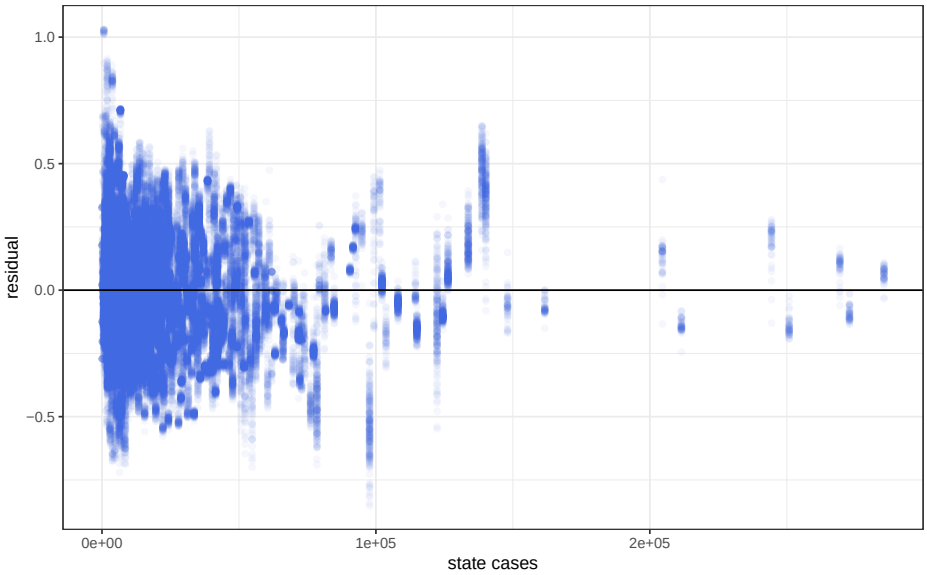

Figure S38. Residuals versus state case incidence demonstrates no clear relationship, suggesting that it is reasonable to exclude state cases from the model.

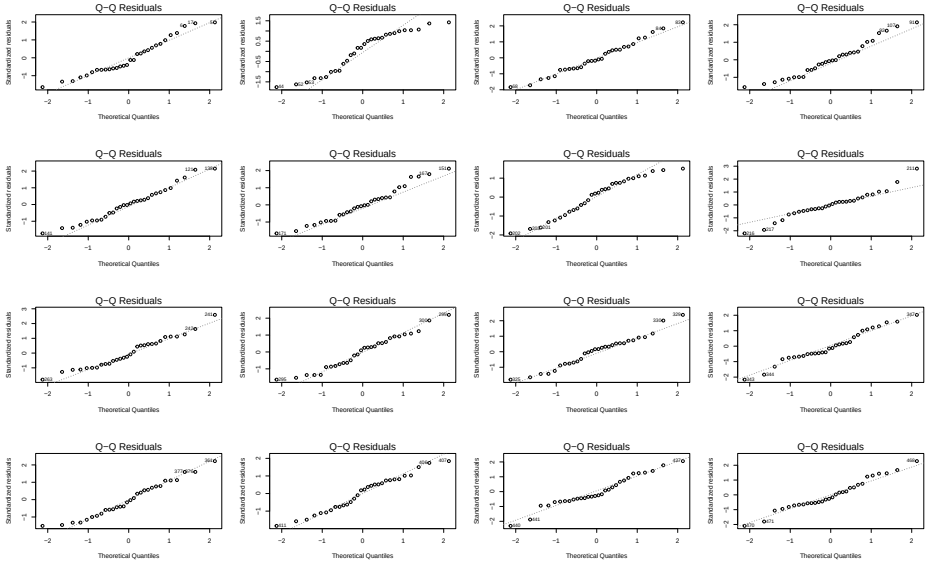

Figure S39. QQ-plots for a random sample of counties demonstrate that residuals are plausibly normal.

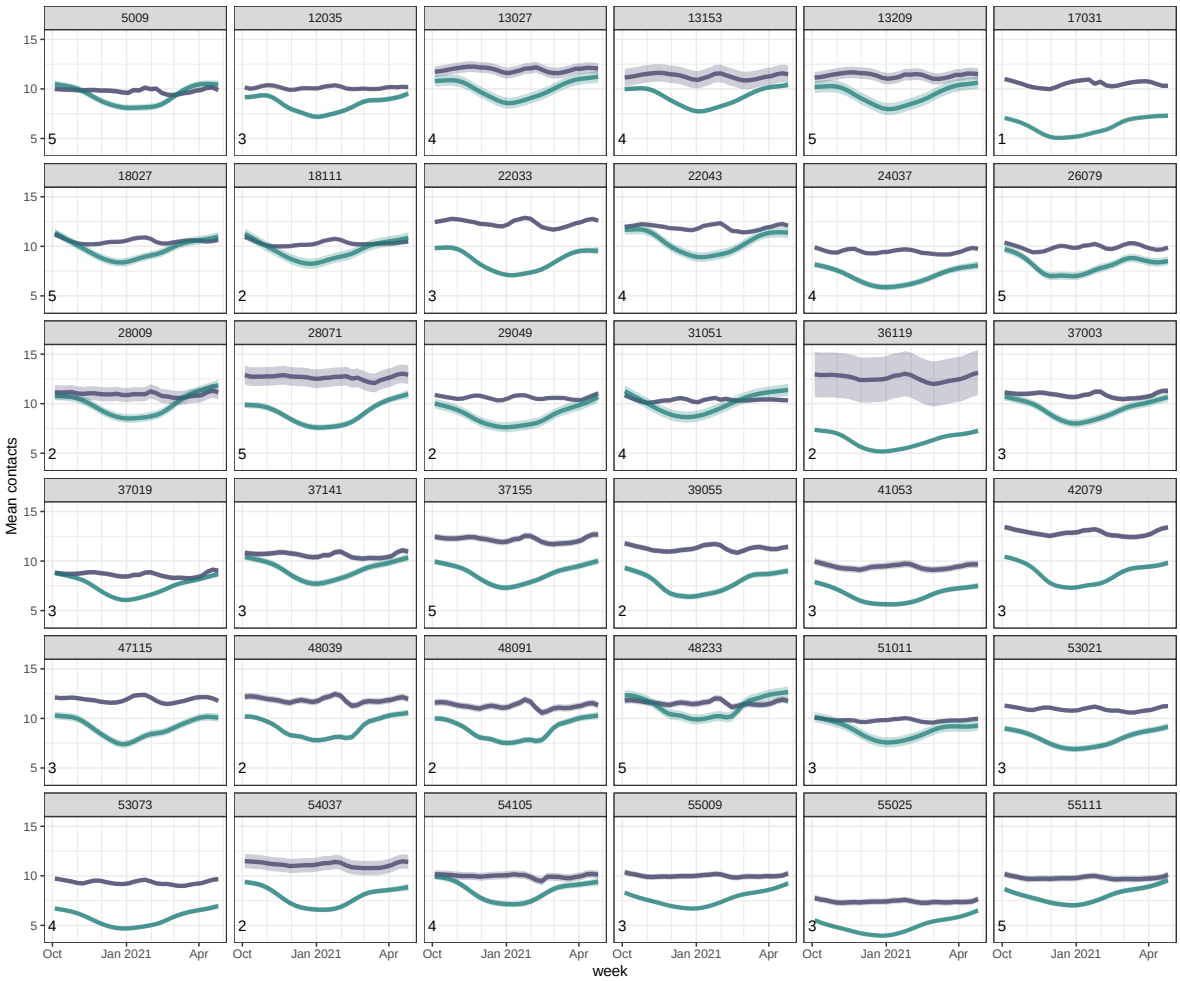

Figure S40. Non-pandemic vs pandemic trajectories for a random sample of counties spanning different urbanicity levels. NCHS classification shown in lower left corner where 1 is urban and 6 rural. Non-pandemic predictions are shown in slate and pandemic estimates are in teal.

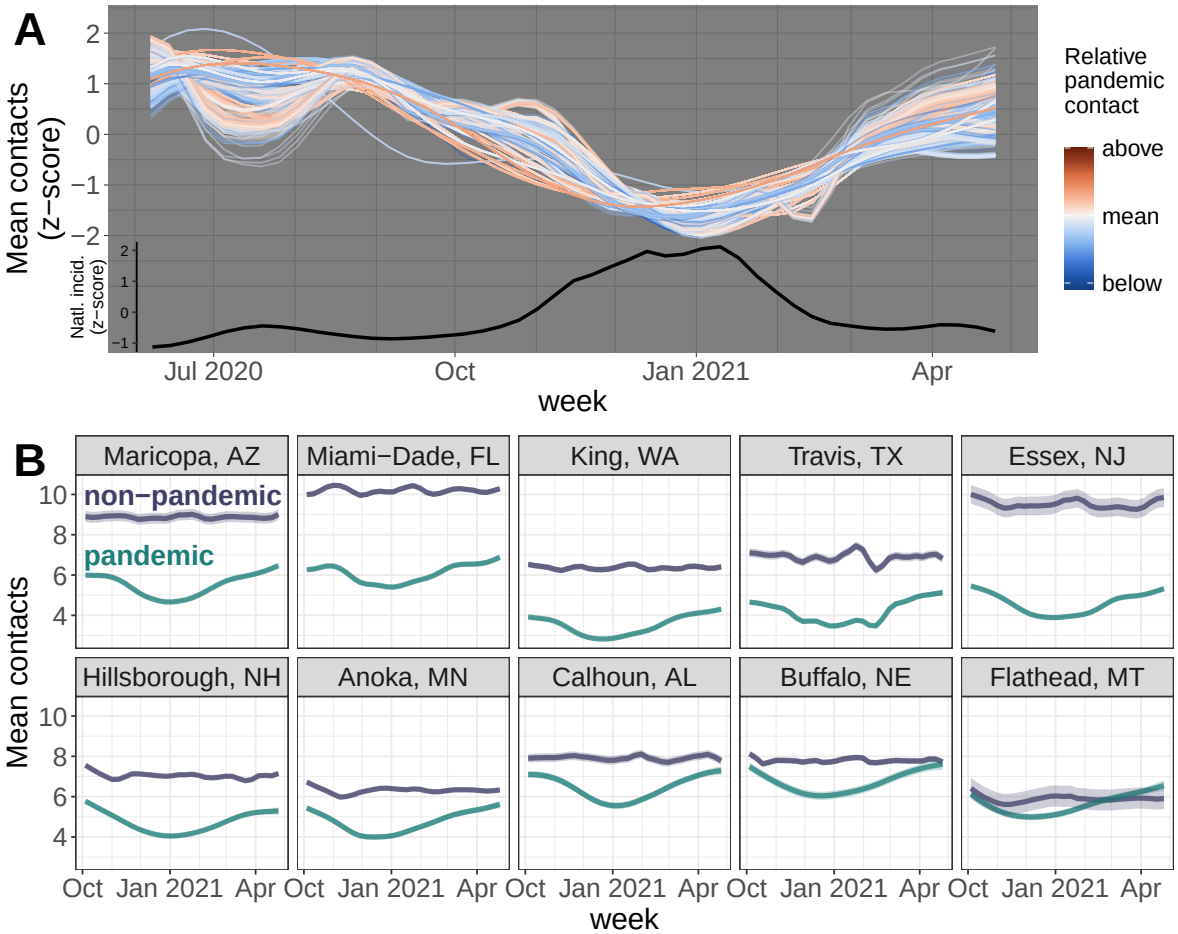

Figure S41. Counties have similar contact dynamics over time and relatively stable contact after controlling for disease using 90th percentile truncation (36 contacts). For more figure details, compare to and see caption for Figure 1 in the main text.

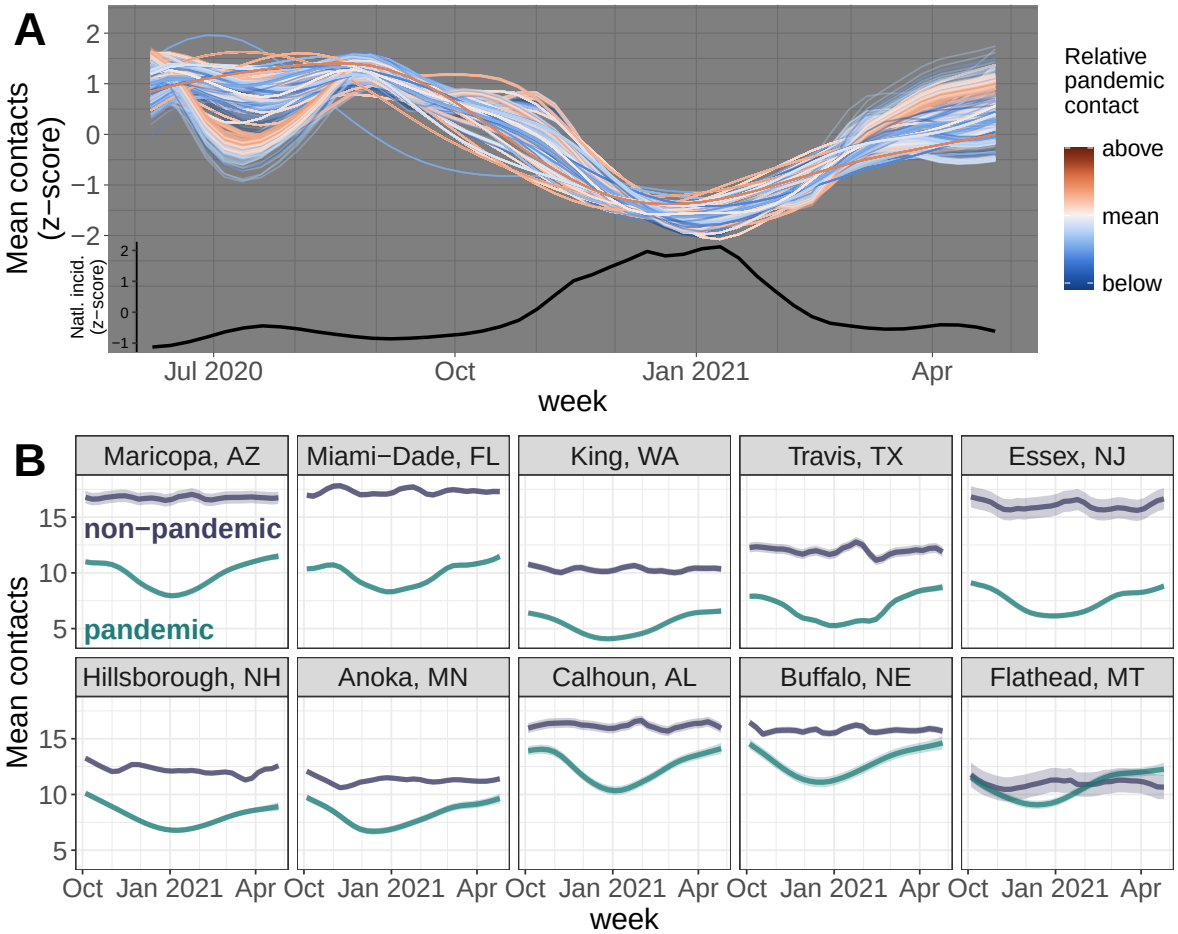

Figure S42. Counties have similar contact dynamics over time and relatively stable contact after controlling for disease using 97th percentile truncation (108 contacts). For more figure details, compare to and see caption for Figure 1 in the main text.

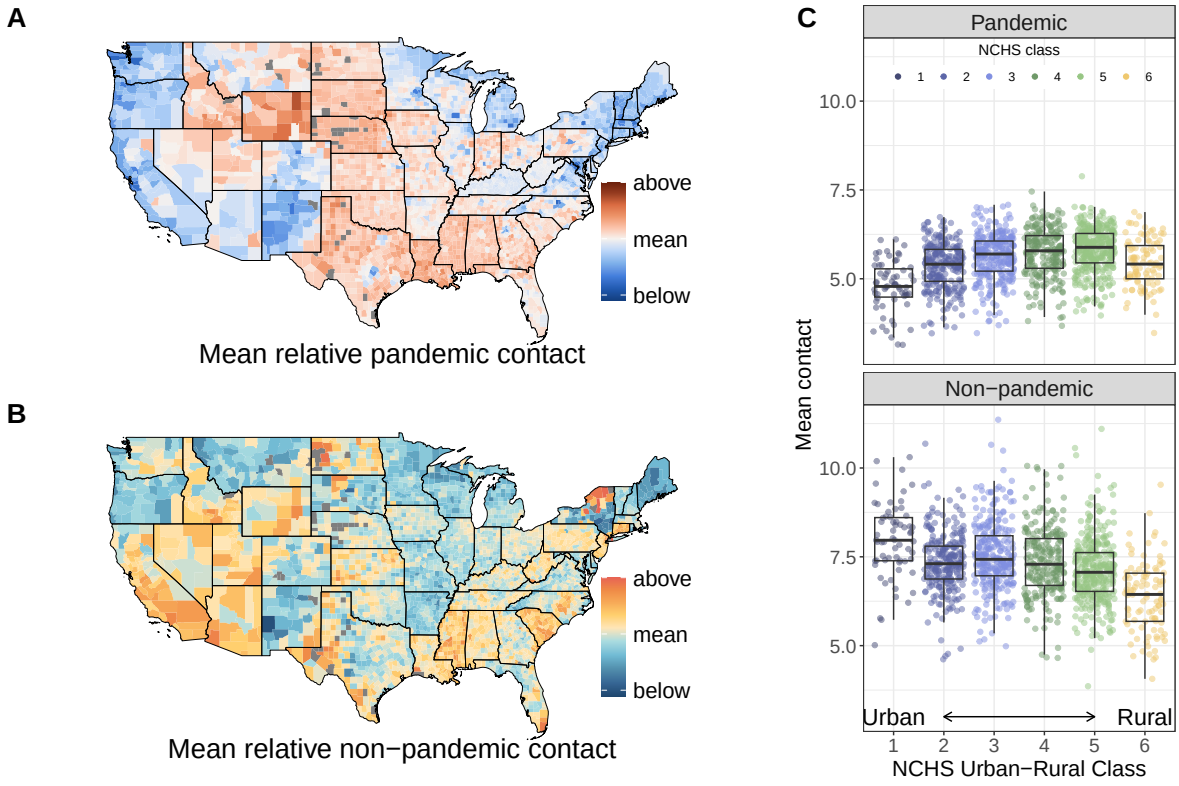

Figure S43. Contact is spatially heterogeneous regardless of disease incidence, but the urban-rural gradient reverses after controlling for disease incidence using 90th percentile truncation point (36 contacts). Reversal of pandemic urban-rural gradient is stronger with this truncation than with the 95th percentile in the main text. For more figure details, compare to and see caption for Figure 2 in the main text.

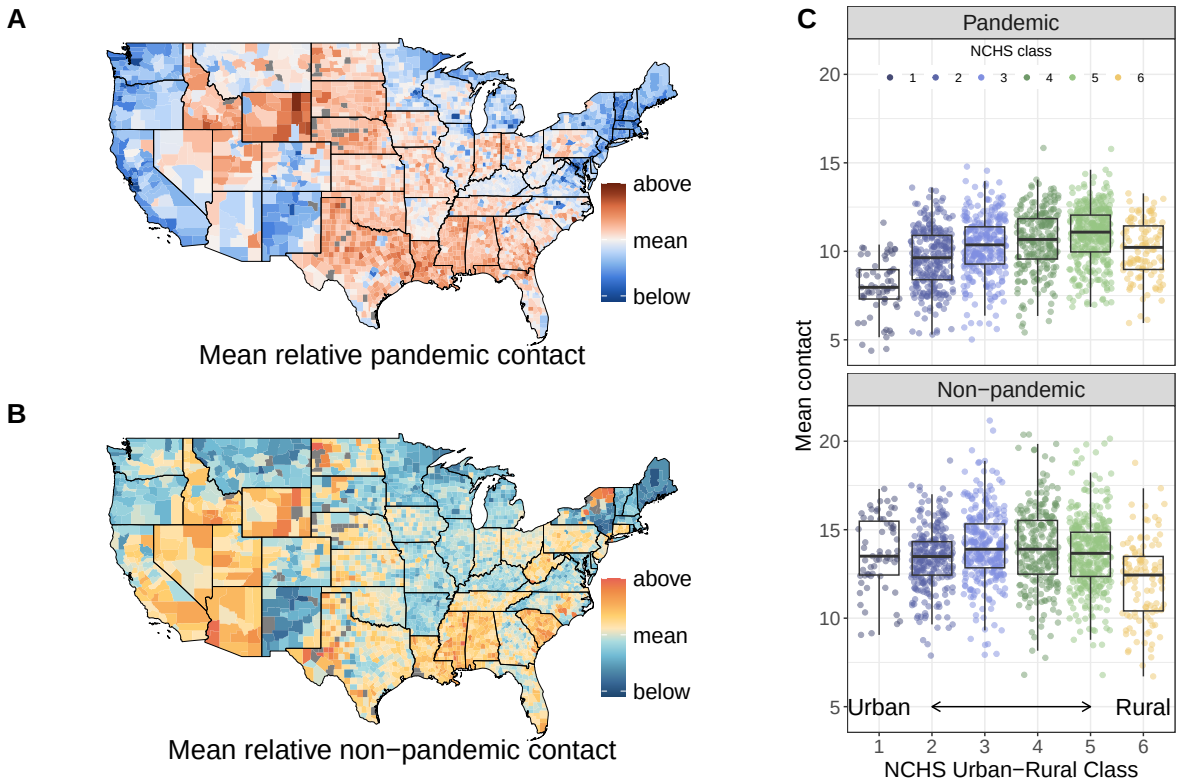

Figure S44. Contact is spatially heterogeneous regardless of disease incidence, but the urban-rural gradient reverses after controlling for disease incidence using 97th percentile truncation point (108 contacts). For more figure details, compare to and see caption for Figure 2 in the main text.

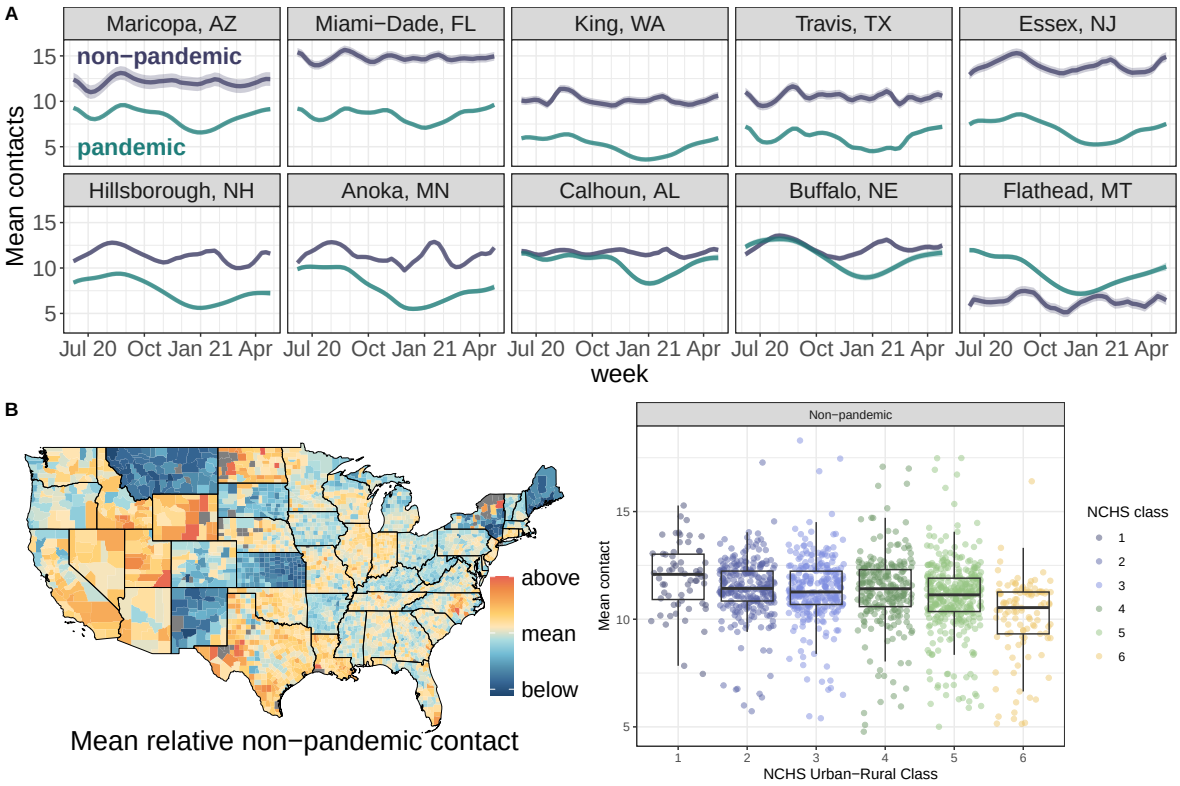

Figure S45. Baseline estimates are less stable when contact data are fit over a longer period (June 2020 - April 2021) with more variation in incidence and policy levels.

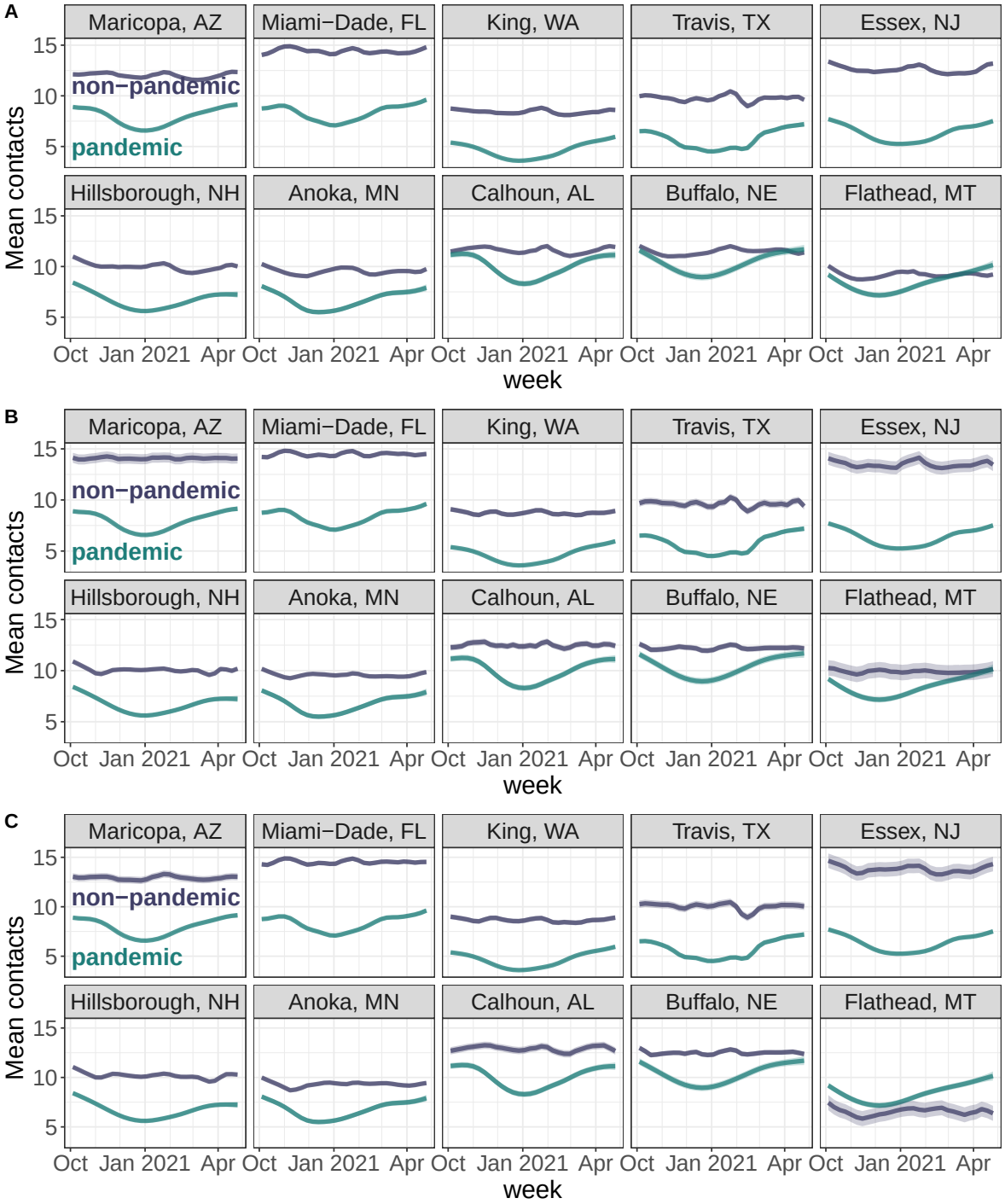

Figure S46. Estimates of baseline contact over time are consistent across different regression models. (A) Model using solely national incident cases and county vaccination coverage, i.e. no policy data. (B) Model incorporating county-level incident cases in addition to covariates in main text model. (C) Same model as main text but without interaction between national incident cases and county vaccination coverage.

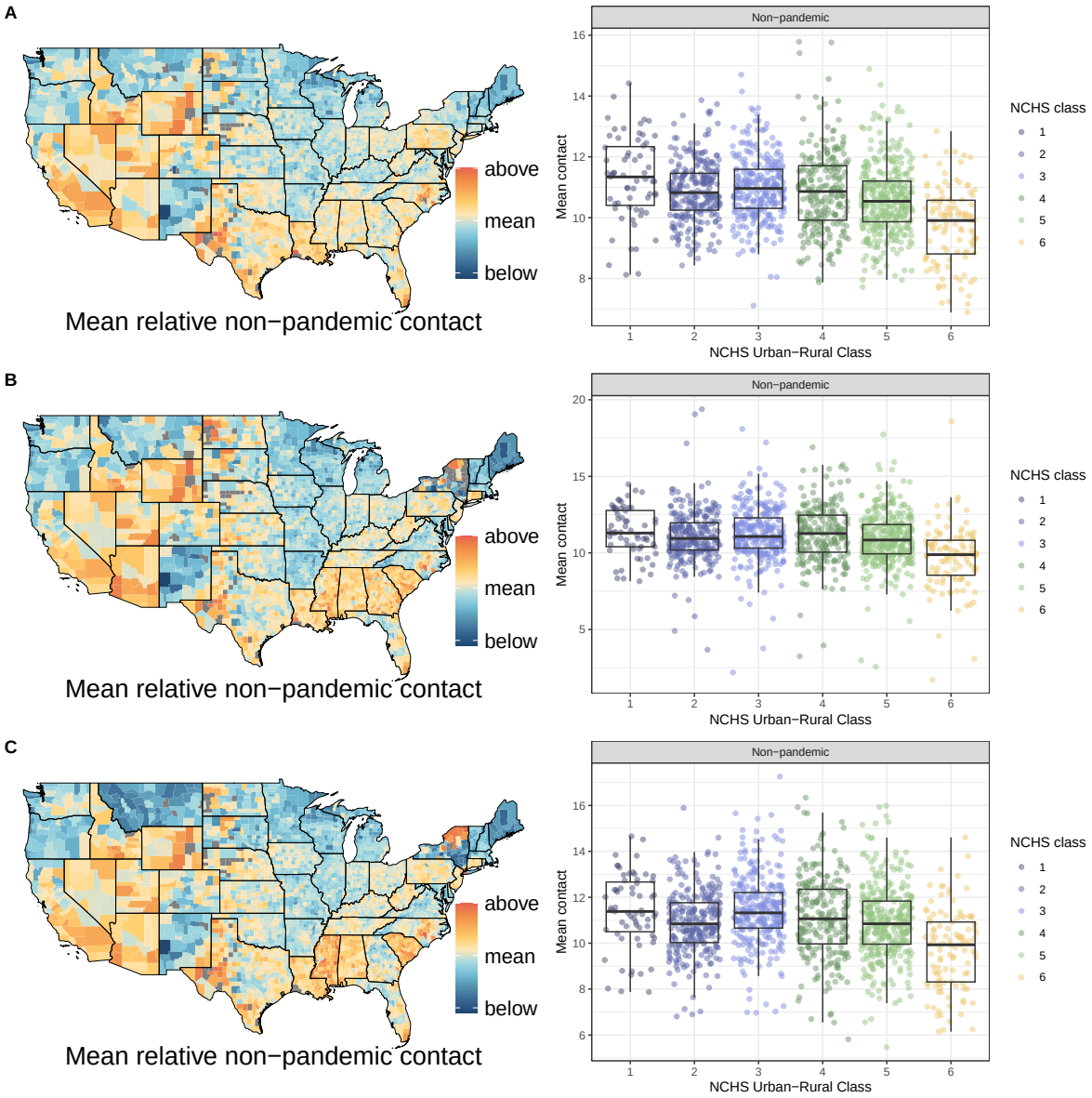

Figure S47. Estimates of baseline contact across space and urbanicity are consistent across different regression models. (A) Model using solely national incident cases and county vaccination coverage, i.e. no policy data. (B) Model incorporating county-level incident cases in addition to covariates in main text model. (C) Same model as main text but without interaction between national incident cases and county vaccination coverage.

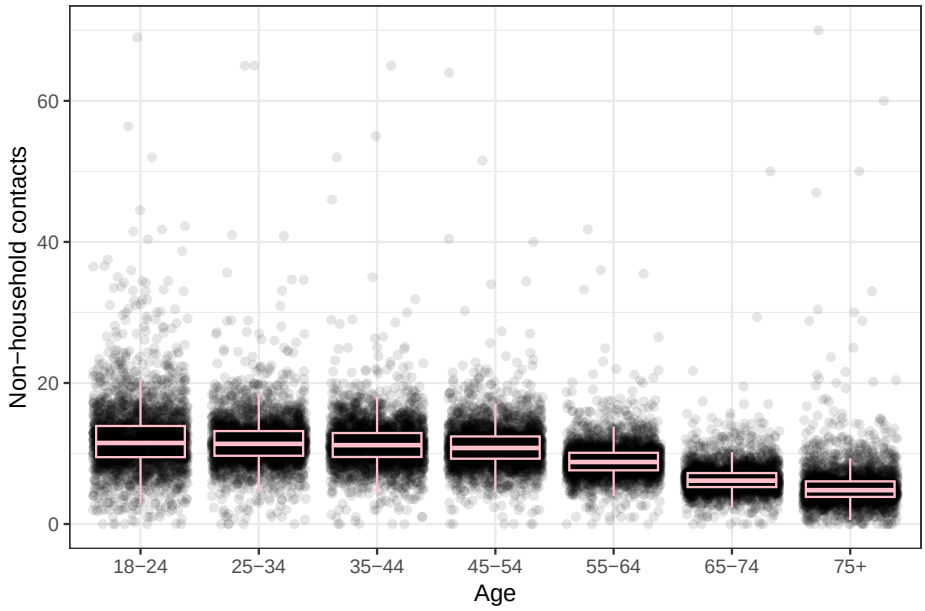

Figure S48. Age groups 18-54 have roughly the same number of contacts. Each point represents a county, raw mean contact for the period June 2020 through April 2021.

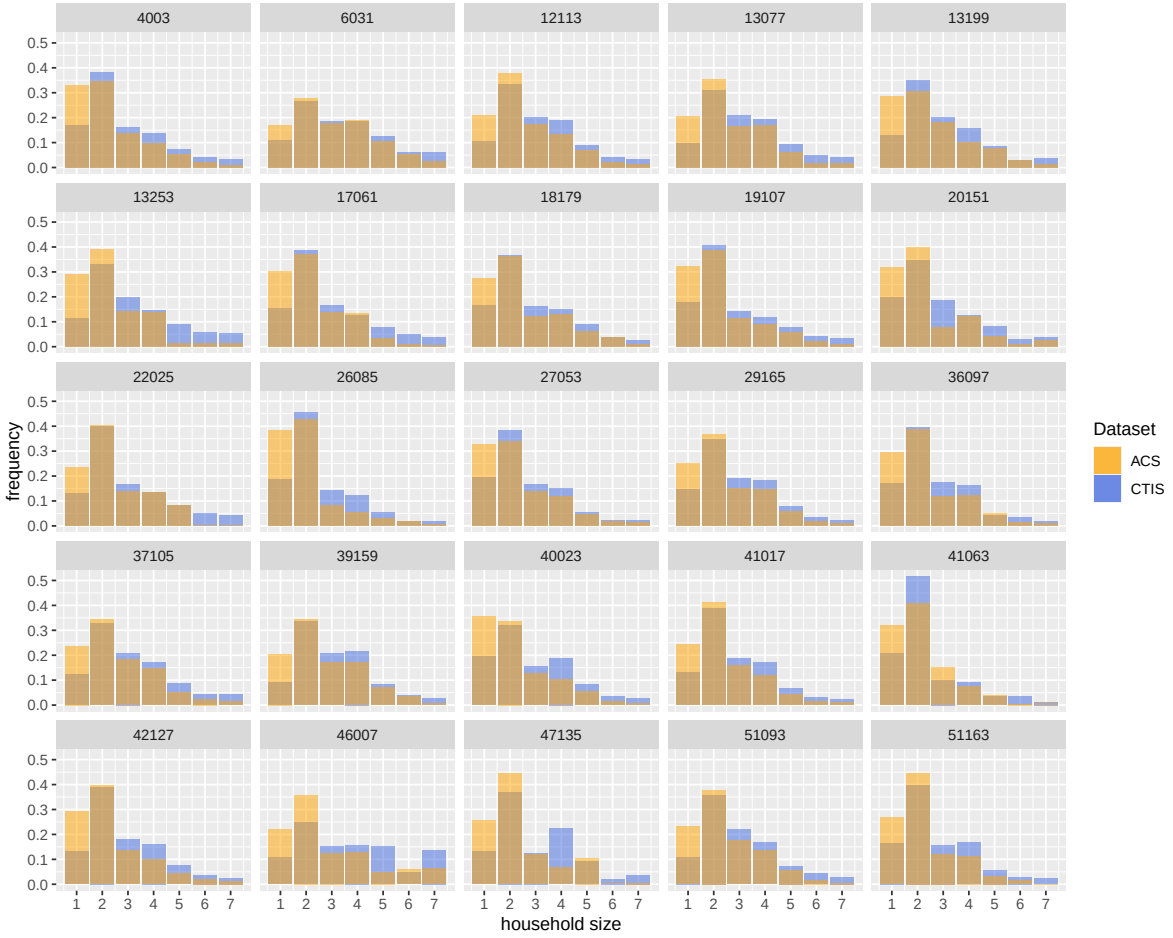

Figure S49. Comparison between household size in raked contact data and census data for a subsample of counties shows that the CTIS decently captures range of household sizes and we do not need to rake on household size. In general, smaller households are underrepresented in the survey and larger households are overrepresented, as expected given that larger households have more people that can respond to the survey.

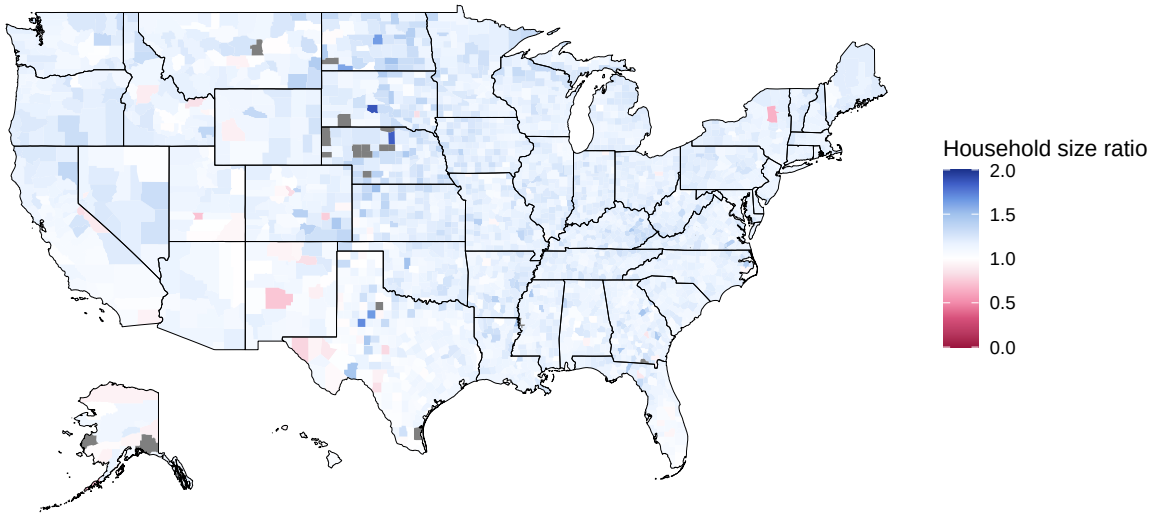

Figure S50. Ratios of mean survey household size and census household size are close to 1.

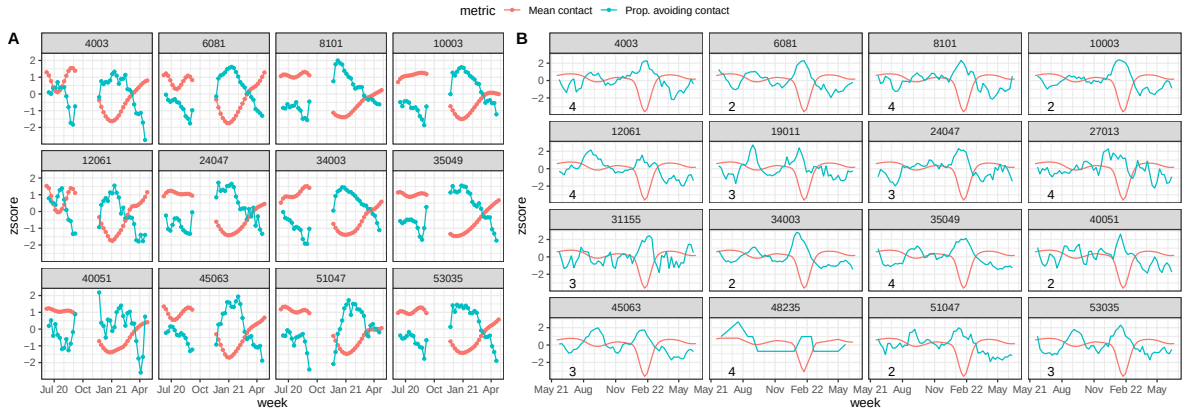

Figure S51. Contact is inversely correlated with the proportion of individuals avoiding contact, as reported in the CTIS. Predicted contact based on national incidence maintains this relationship with observed avoidance data. (A) Z-scored centered 3-week rolling average of raw proportions of respondents avoiding contact compared to z-scored GAM-estimated contact. The question about avoiding contacts was omitted from the CTIS from Step 8, 2020 to November 24, 2020, hence the gap in data. (B) Predicted contact (based only on national case incidence) compared to reported proportion avoiding contact on the CTIS from May 2021 through the end of the survey in June 2022.

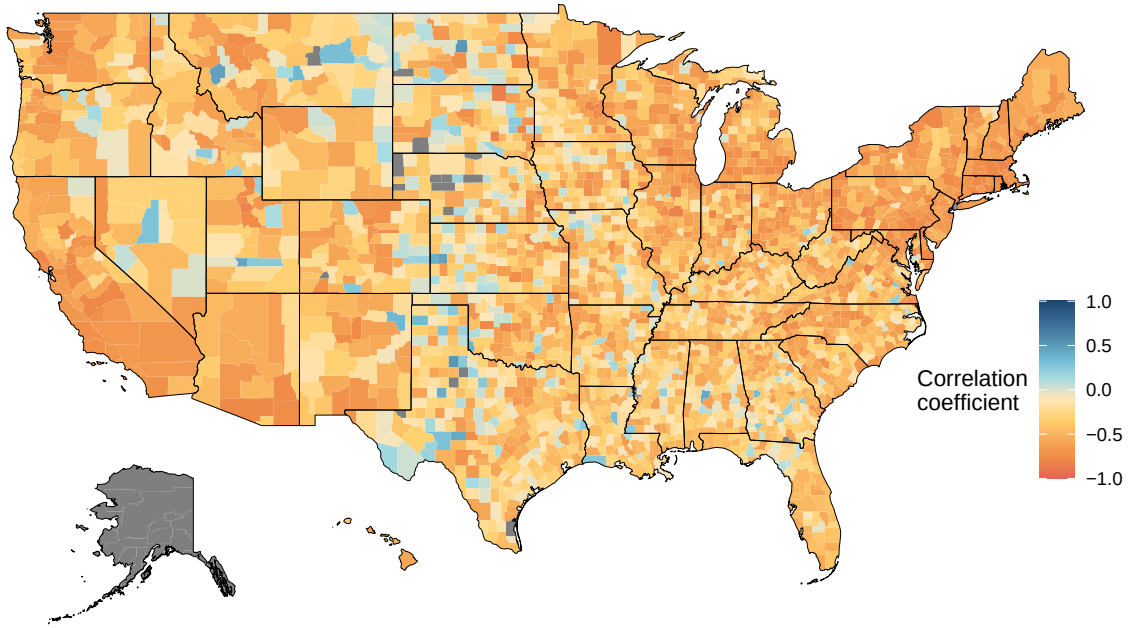

Figure S52. Correlation between predicted out of sample contact and observed contact avoidance across counties. Contact avoidance is calculated as the centered 3-week rolling average of raw proportions of respondents avoiding contact while predicted contact is based only on national incidence from May 2021 through the end of the survey in June 2022. Mean Pearson's correlation is -0.40 (sd = 0.23).

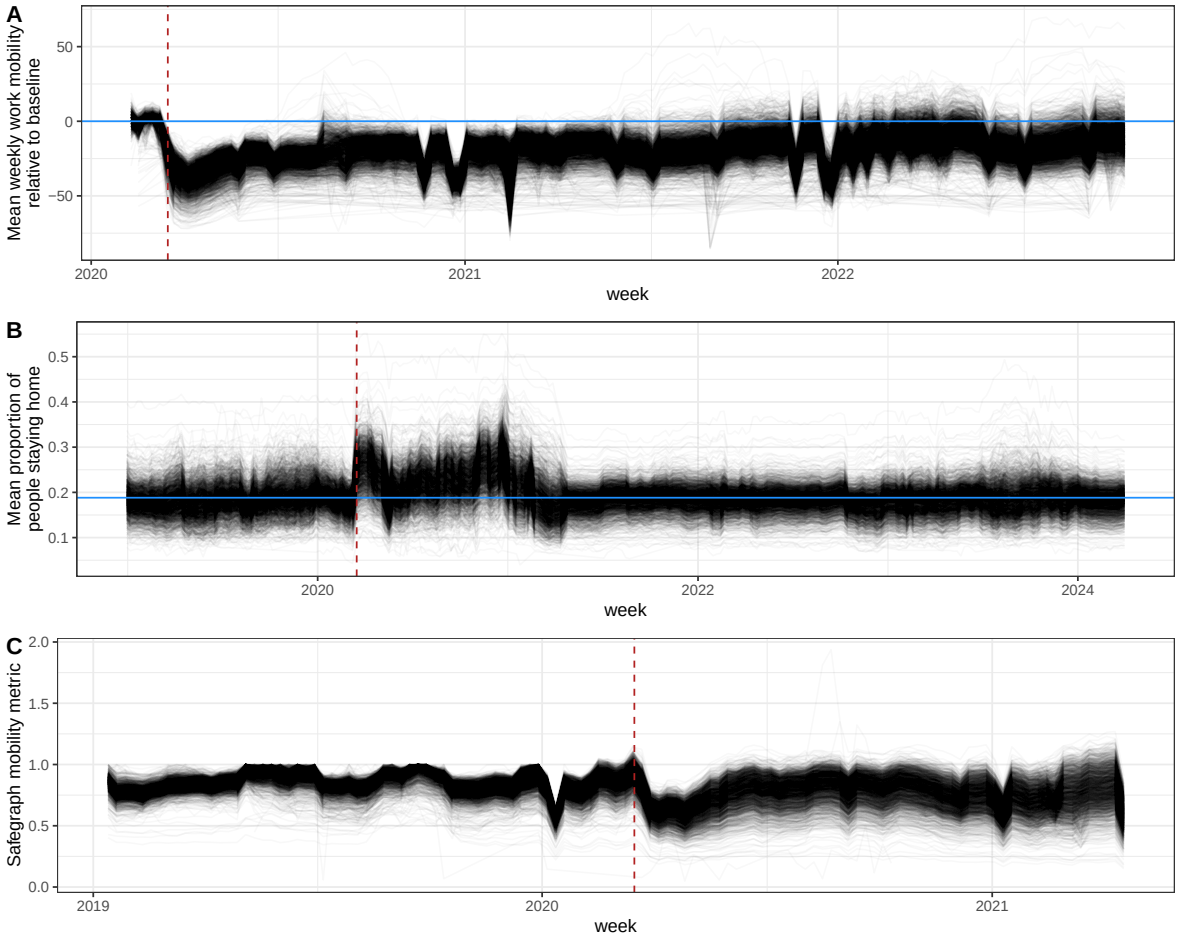

Figure S53. Mobility time series show precipitous drop in mobility in March 2020 and return to near normal levels towards the end of 2022. (A) Mean weekly work mobility relative to baseline from Google [70]. (B) Bureau of Transportation Statistics mean proportion of people staying home [71]. (C) Safegraph Social Distancing Dataset mobility metric [44].

Supplemental References

56. Meta. User Guide for the COVID-19 Trends and Impact Survey Weights; 2022. Version 1.

57. Salomon JA, Reinhart A, Bilinski A, Chua EJ, La Motte-Kerr W, Rönn MM, et al. The US COVID-19 Trends and Impact Survey: Continuous Real-Time Measurement of COVID-19 Symptoms, Risks, Protective Behaviors, Testing, and Vaccination. Proceedings of the National Academy of Sciences. 2021 Dec;118(51):e2111454118.

58. Pasek J. Anesrake: ANES Raking Implementation; 2018. https://CRAN.R-project.org/package=anesrake.

59. Wood SN. Generalized Additive Models: An Introduction with R. Second edition ed. Chapman & Hall/CRC Texts in Statistical Science. Boca Raton: CRC Press/Taylor & Francis Group; 2017.

60. Mossong J, Hens N, Jit M, Beutels P, Auranen K, Mikolajczyk R, et al. Social Contacts and Mixing Patterns Relevant to the Spread of Infectious Diseases. PLOS Medicine. 2008 Mar;5(3):e74.

61. DeStefano F, Haber M, Currivan D, Farris T, Burrus B, Stone-Wiggins B, et al. Factors Associated with Social Contacts in Four Communities during the 2007–2008 Influenza Season. Epidemiology & Infection. 2011 Aug;139(8):1181–1190.

62. Feehan DM, Cobb C. Using an Online Sample to Estimate the Size of an Offline Population. Demography. 2019 Dec;56(6):2377–2392.

63. Nelson KN, Siegler AJ, Sullivan PS, Bradley H, Hall E, Luisi N, et al. Nationally Representative Social Contact Patterns among U.S. Adults, August 2020-April 2021. Epidemics. 2022 Sep;40:100605.

64. Dorélien AM, Venkateswaran N, Deng J, Searle K, Enns E, Alarcon Espinoza G, et al. Quantifying Social Contact Patterns in Minnesota during Stay-at-Home Social Distancing Order. BMC Infectious Diseases. 2023 May;23(1):324.

65. Feehan DM, Mahmud AS. Quantifying Population Contact Patterns in the United States during the COVID-19 Pandemic. Nature Communications. 2021 Feb;12(1):893.

66. Kiti MC, Aguolu OG, Zelaya A, Chen HY, Ahmed N, Batross J, et al. Changing Social Contact Patterns among US Workers during the COVID-19 Pandemic: April 2020 to December 2021. Epidemics. 2023 Dec;45:100727.

67. Breen CF, Mahmud AS, Feehan DM. Novel Estimates Reveal Subnational Heterogeneities in Disease-Relevant Contact Patterns in the United States. PLOS Computational Biology. 2022 Dec;18(12):e1010742.

68. Crawford FW, Jones SA, Cartter M, Dean SG, Warren JL, Li ZR, et al. Impact of Close Interpersonal Contact on COVID-19 Incidence: Evidence from 1 Year of Mobile Device Data. Science Advances. 2022 Jan;8(1):eabi5499.

69. Hale T, Angrist N, Goldszmidt R, Kira B, Petherick A, Phillips T, et al. A Global Panel Database of Pandemic Policies (Oxford COVID-19 Government Response Tracker). Nature Human Behaviour. 2021 Apr;5(4):529–538.

70. Google. COVID-19 Community Mobility Report; 2021. https://www.google.com/covid19/mobility?hl=en.

71. Daily Travel | Bureau of Transportation Statistics;. https://www.bts.gov/daily-travel.

72. Safegraph. Social Distancing Metrics;. https://docs.safegraph.com/docs/social-distancing-metrics.